

ISSET JOURNAL OF EARTHQUAKE TECHNOLOGY

Vol. 45

No. 1-2

March-June 2008

CONTENTS

No.	Paper	Page
494	Influence of Liquefaction on Pile-Soil Interaction in Vertical Vibration B.K. Maheshwari, U.K. Nath and G. Ramasamy	1
495	<u>28th ISET ANNUAL LECTURE</u> Foundations for Industrial Machines and Earthquake Effects K.G. Bhatia	13
496	Numerical Analysis of Performance of Soil Nail Walls in Seismic Conditions G.L. Sivakumar Babu and Vikas Pratap Singh	31

Financial Assistance from AICTE and DST, New Delhi for the Publication of ISET Journals for 2007–2008 and 2008–2009 is duly acknowledged.

INFLUENCE OF LIQUEFACTION ON PILE-SOIL INTERACTION IN VERTICAL VIBRATION

B.K. Maheshwari*, U.K. Nath** and G. Ramasamy***

*Department of Earthquake Engineering, IIT Roorkee, Roorkee-247667

**Department of Civil Engineering, Jorhat Engineering College, Jorhat-285007

***Department of Civil Engineering, IIT Roorkee, Roorkee-247667

ABSTRACT

During strong earthquake shaking, loose cohesionless soils below the water table develop high pore water pressures and liquefy leading to significant degradation of strength and stiffness. In such soil stratum, pile foundations may undergo substantial shaking while the soil is in a fully liquefied state and soil stiffness is at its minimum. In this paper, an available numerical model formulating the pore pressure response directly from observed data on undrained tests has been used to study the liquefaction phenomenon. The Winkler soil model has been used to model the pile-soil interaction. Combining these two models, a formulation to predict the response of a pile in liquefiable soils in axial vibration is developed. It is observed that the response of a single pile due to axial vibration in liquefiable soil is significantly greater than that in non-liquefiable soil, particularly at higher frequencies.

KEYWORDS: Pile-Soil Interaction, Liquefaction, Winkler Soil Model, Numerical Models

INTRODUCTION

Damage to buildings, bridges, port facilities and other infrastructure during several major earthquakes has warranted attention of researchers towards the behavior of foundations under dynamic loading. Although studies of seismic loading of piles and of liquefaction phenomenon have been performed over the last four decades, the combined problem of seismic behavior of piles in liquefiable soil has received relatively less attention. Several experimental and analytical studies of this combined problem have been presented in the last five years (Finn and Fujita, 2002; Liyanapathirana and Poulos, 2005; Miwa et al., 2006). Yet much has to be revealed especially regarding the key aspects of influence of flow characteristic on this behavior. The excess pore pressure generated during liquefaction alters effective stresses in the soil and changes its mechanical behavior. The numerical formulation of the problem significantly reduces the computational effort needed for the solution.

During strong ground motion, piles are prone to severe cracking or even fracture. Liquefaction leads to substantial increase in the pile-cap displacements. After liquefaction, if the residual strength of the soil is less than the static shear stresses caused by a sloping site or a free surface such as a river-bank, significant lateral spreading or down-slope displacements may occur (Finn and Fujita, 2002). The moving soil can exert damaging pressures against the piles, leading to failure. Such failures were prevalent during the 1964 Niigata and the 1995 Kobe earthquakes. Seed and Idriss (1971), Martin and Seed (1979) observed the liquefaction phenomenon extensively and their model was based on the effective stress concept. Martin et al. (1975) showed that under drained conditions, loose sand would compact due to shearing.

Novak (1974) was first to use a Winkler model for the representation of a laterally loaded pile in a visco-elastic material. In Novak's solution, the soil is composed of horizontal layers that are homogenous, isotropic and linearly elastic. The soil reaction at any depth is that of an infinitely long rigid pile undergoing uniform harmonic vibration in an infinite medium and the plane strain conditions are assumed to hold. The pile foundations are subjected to axial vibration in many situations such as loading due to machinery and during earthquakes. Most of the initial reported research work on the soil-pile interaction was for vertical vibration. Nogami and Konagai (1986) and Konagai and Nogami (1987) suggested a simple mechanical model, which approximates the frequency-dependent behavior of plane-strain Winkler model used by Novak et al. (1978). El Naggar and Novak (1994) presented nonlinear soil model for axial pile response. Maheshwari et al. (2005) included the effects of soil plasticity while analyzing the soil-pile interaction.

The combined problem of pile-soil interaction and liquefaction has been studied only in the last decade. The measurements of dynamic p - y behavior for liquefying sand were presented by Wilson (1998), based on back-analyses of dynamic centrifuge model tests (Katsuichiro et al., 2004). Bhattacharya et al. (2004) reported buckling instability of pile foundations in liquefiable ground in axial direction. A pseudo-static approach has been adopted by Liyanapathirana and Poulos (2005), which involves two main steps. First, they carried out a nonlinear free-field site response analysis to obtain the maximum ground displacements along the pile and the degraded soil modulus over the depth of the soil deposit. In the second step, a static load analysis based on the maximum ground surface acceleration is performed.

The objective of this paper is to evaluate the response of a pile subjected to axial vibration in liquefiable soil taking into account the effects of pile-soil interaction. The analysis has been performed in the time domain. The degradation of the soil shear strength due to liquefaction is modeled using the numerical model proposed by Seed et al. (1976) and modified by Liyanapathirana and Poulos (2002a). Pile-soil interaction is incorporated in the model using the methodology suggested by Nogami and Konagai (1986) and extended by Konagai and Nogami (1987). Using this new methodology, the response of pile in liquefiable soils is predicted (Nath, 2006). Here, only a single end-bearing pile is considered. However, the model is capable of dealing with a pile group.

NUMERICAL FORMULATION

This is presented separately for liquefaction and for pile-soil interaction.

1. Modeling for Liquefaction

1.1 Zone of Liquefaction

It is important to check whether, for a given condition, the soil stratum liquefies. The first step in the analysis is to find the zone of liquefaction. This is determined by comparing the average shear stress τ_{av} due to earthquake loading and the shear stress τ causing liquefaction. The average shear stress is given by (Seed and Idriss, 1971)

$$\tau_{av} = 0.65 \frac{a_{\max}}{g} \sigma_v r_d \quad (1)$$

where, a_{\max} is the peak ground acceleration, σ_v is the total overburden pressure, and r_d is the depth reduction factor. The shear stress causing liquefaction is given by (Prakash, 1981)

$$\left(\frac{\tau}{\sigma'_v} \right)_{D_r} = \left(\frac{\sigma_{dc}}{2\sigma_a} \right)_{50} C_r \frac{D_r}{50} \quad (2)$$

where, $(\sigma_{dc}/2\sigma_a)_{50}$ is the cyclic stress ratio (CSR), which can be found from the charts (Seed and Idriss, 1971), provided D_{50} of the soil is known. The charts are prepared on the basis of a number of cyclic triaxial and simple shear tests. Separate charts are applicable for different numbers of cycles causing liquefaction, which, in turn, depend on the magnitude of the earthquake. Further, in Equation (2), D_r denotes the relative density of soil in percentage, and C_r is a correction factor, the value of which depends on D_r .

1.2 Numerical Model

The numerical modeling for the liquefaction of soil is based on Seed et al. (1976), and Liyanapathirana and Poulos (2002a). The three basic steps are evaluation of (a) rate of pore pressure generation, (b) pore pressure redistribution and dissipation, and (c) the stress response analysis with pore water pressure induced. These steps of numerical formulation are discussed in detail in Liyanapathirana and Poulos (2002a, 2002b), and are briefly described here.

Rate of Pore Pressure Generation, $\partial u_g / \partial t$: The rate of pore pressure generation during earthquake shaking is calculated as follows (Liyanapathirana and Poulos, 2002a):

$$\frac{\partial u_g}{\partial t} = \frac{\partial u_g}{\partial N} \frac{\partial N}{\partial t} = \frac{\sigma'_{v0}}{\theta \pi N_L \sin^{2\theta-1}(\pi r_p / 2) \cos(\pi r_p / 2)} \frac{\partial N}{\partial t} \quad (3a)$$

where, u_g is the excess pore pressure generated due to earthquake loading; $\partial N / \partial t$ is the rate of application of shear stress cycles to the soil; σ'_{v0} is the initial effective overburden pressure; and r_p is the pore pressure ratio, i.e., the ratio of excess pore water pressure to initial effective overburden pressure. The shear stress rate $\partial N / \partial t$ can be worked out by first representing the actual stress time-history into an equivalent number N_{eq} of uniform stress cycles (Seed et al., 1976). For harmonic excitation, $\partial N / \partial t$ is simply the frequency of excitation. The value of r_p is given by the following expression:

$$r_p = \frac{u_g}{\sigma'_{v0}} = \frac{2}{\pi} \sin^{-1} \left(\frac{N}{N_L} \right)^{\frac{1}{2\theta}} \quad (3b)$$

where, N_L is the number of uniform stress cycles required to produce a condition of initial liquefaction (i.e., excess pore pressure = effective confining pressure) under undrained conditions. The value of N_L can be read off from a family of curves (which are developed based on simple shear tests) as discussed by Seed et al. (1976). Further, N is the number of equivalent uniform cycles, for harmonic excitation $N = N_{eq}$, and can be worked with the magnitude of earthquake. The parameter θ is assumed as 0.7 in the analysis for the best fit.

Pore Pressure Redistribution and Dissipation: Considering pore pressure distribution within the soil due to vertical drainage, the net excess pore pressure $\partial u / \partial t$ developed in the soil, in one-dimensional formulation, is given by (Liyanapathirana and Poulos, 2002a)

$$\frac{\partial u}{\partial t} = \frac{1}{m_v \gamma_w} \frac{\partial}{\partial z} \left(k \frac{\partial u}{\partial z} \right) + \frac{\partial u_g}{\partial t} \quad (3c)$$

where, k is the permeability of the soil, m_v is the tangent coefficient of volume compressibility, γ_w is the unit weight of water, and $\partial u / \partial z$ is the gradient of excess pore pressure in the vertical direction. The value of m_v is given by the following expression:

$$\frac{m_v}{m_{v0}} = \frac{e^{ar_p^b}}{1 + ar_p^b + 0.5a^2 r_p^{2b}} \quad (3d)$$

where, m_{v0} is the tangent coefficient of volume compressibility at low pressure. The values of a and b are dependent on relative density of soil D_r and can be expressed as follows:

$$a = 5(1.5 - D_r) \quad \text{and} \quad b = (3/2)^{2D_r} \quad (3e)$$

The value of m_{v0} may be taken as $26.1 \times 10^{-6} \text{ m}^2/\text{kN}$ and $41.8 \times 10^{-6} \text{ m}^2/\text{kN}$ for dense and loose soil, respectively (Seed et al., 1976).

Effective Stress Response Analysis with Pore Water Pressure Induced: Using Equation (3a) (for $N_{eq} < N_L$) generated pore water pressure, or using Equation (3c) (for $N_{eq} > N_L$ with $r_p = 1$), redistributed pore water pressure is determined. Thus the excess pressure, and in turn the effective stress, can be worked out. At the end of each loading and reloading phase, the soil stiffness is degraded based on the effective stress in the soil as (Liyanapathirana and Poulos, 2002a)

$$\frac{G_t}{G_0} = \left(\frac{\sigma'_{vt}}{\sigma'_{v0}} \right)^\eta \quad (3f)$$

Here G_t , G_0 , σ'_{vt} and σ'_{v0} are the shear modulus at time t , the initial shear modulus, the effective overburden stress at time t , and the initial effective overburden stress, respectively. Further, η is the

power exponent and is generally equal to 0.5. The shear strength of the soil is also modified progressively as

$$\frac{\tau_{ft}}{\tau_{f0}} = \left(\frac{\sigma'_{vt}}{\sigma'_{v0}} \right)^\eta \tag{3g}$$

2. Modeling for Pile-Soil Interaction

First, configuration of the soil-pile system is discussed, followed by numerical modeling.

2.1 Configuration of the System

The configuration of the soil-pile system is shown in Figure 1. It is assumed that there is a hard stratum either at the pile tip or at some depth below the tip, so that piles which are not directly resting on the bedrock can be analyzed using the same methodology as the end-bearing piles by assuming a fictitious pile, made of soil below the pile tip. The pile-soil system is divided into horizontal slices containing the pile segment and homogenous soil layer. The Winkler soil model units are assumed to be uniformly distributed along the pile shaft for modeling the soil medium around the pile.

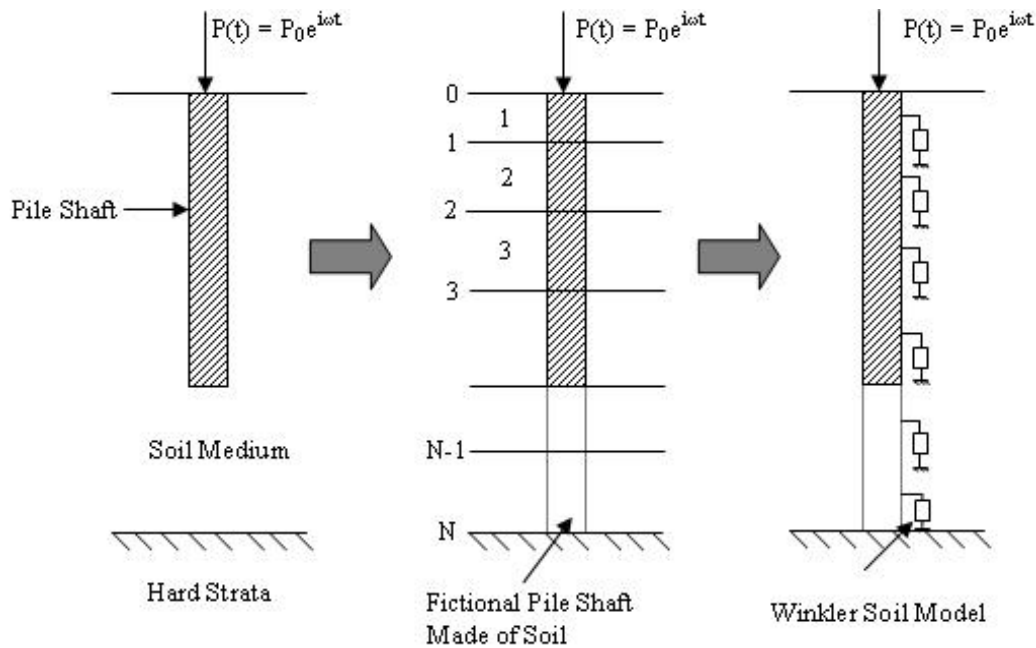


Fig. 1 Soil-pile system divided into horizontal slices

One unit of model is shown in Figure 2; this is shown in horizontal direction for convenience, although it is attached to the pile in the vertical direction.

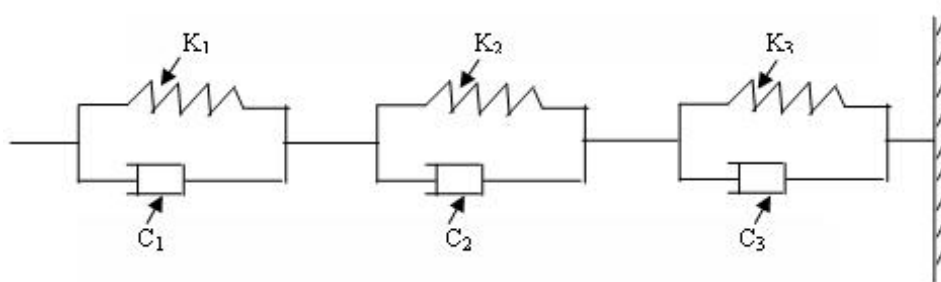


Fig. 2 One unit of Winkler soil model for the axial pile shaft response (shown in the horizontal direction for convenience; this is actually attached to the pile in the vertical direction)

For the axial loading, the values of the model parameters are determined using the following expressions (Nogami and Konagai, 1986):

$$(k_1, k_2, k_3) = G_s(3.518, 3.581, 5.529) \quad (4a)$$

$$(c_1, c_2, c_3) = \frac{G_s r_0}{V_s}(113.097, 25.133, 9.362) \quad (4b)$$

Here G_s , r_0 , and V_s are shear modulus, radius of embedded pile, and shear wave velocity of the soil, respectively. It may be noted that these parameters are frequency-independent.

2.2 Numerical Modeling

The numerical model for vertical vibration (Nogami and Konagai, 1986) is based on Winkler's hypothesis, i.e., the soil-pile interaction force is related to the pile-shaft displacements only at that depth where the interaction force is considered. The pile-soil system is divided into number of layers (see Figure 1). Applying the boundary conditions at the two adjacent segments, the displacements and forces at the bottom of the n th segment of the pile shaft or soil column can be calculated as (Nogami and Konagai, 1986)

$$\begin{Bmatrix} w_i \\ P_i \end{Bmatrix}_n = [T_n] \begin{Bmatrix} w_i \\ P_i \end{Bmatrix}_0 + \{Q_n\} \quad (4c)$$

where,

$$[T_1] = [t_1] \text{ and } \{Q_1\} = [q_1] \{\gamma_{i,1}\} \text{ for } n = 1 \quad (4d)$$

and

$$[T_n] = [t_n][T_{n-1}] \text{ and } \{Q_n\} = [t_n]\{Q_{n-1}\} + [q_n]\{\gamma_{i,n}\} \text{ for } n \geq 2 \quad (4e)$$

Here w_i and P_i are the axial pile displacement and applied axial load, respectively, and n indicates the number of layer. Also $[t]$ and $[q]$ are 2×2 matrices which are dependent on the material and geometrical properties of the pile, while γ_i is a vector. Details of these matrices and vector can be found in Nogami and Konagai (1986). The values of G_s are considered as G_0 and G_l (as obtained from Equation (3f)) for the analysis of pile-soil interaction in non-liquefiable soil and liquefiable soil, respectively.

Equations (4a)–(4e) are for a single pile; Konagai and Nogami (1987) extended this methodology for a pile group where displacement in soil at distance r from the source of disturbance (i.e., the pile axis) can be found. Thus shear strain, and in turn shear stress, developed in the soil medium due to vertical vibration can be estimated. Here it should be noted that soil is modeled using Winkler soil model which treats soil as a visco-elastic material, and that parameters are given by Equations (4a) and (4b). Further, no plasticity or yielding of soil is considered, though degradation of the material is taken into account using Equation (3f), which is based on the effective stress principle. An advanced plasticity-based model could also be considered.

VERIFICATION OF THE MODELS

Since a rigorous approach has been chosen for the soil-pile interaction and liquefaction analysis, verification of the models and computation technique is imperative. This is performed by comparing the results obtained from the present analysis with well-established results in literature. It may be noted that no commercial software has been used for the computations, and that a computer code has been developed in C++ language to compute the results presented here.

1. Verification for Complex Soil Stiffness

Modeling of the pile-soil interaction for axial load has been carried out using Winkler's hypothesis. A concrete pile of diameter 1 m, length 20 m, and fixed at the pile tip is considered. Figure 3 shows variation in dimensionless complex soil stiffness with dimensionless frequency a_0 ($= \omega r_0 / V_s$) due to the application of axial load. It can be observed that the real part remains relatively constant with frequency while the imaginary part is linearly increasing. These trends of results are in very good agreement with

those presented by Nogami and Konagai (1986) and shown in Figure 3. This verifies the computational algorithm developed.

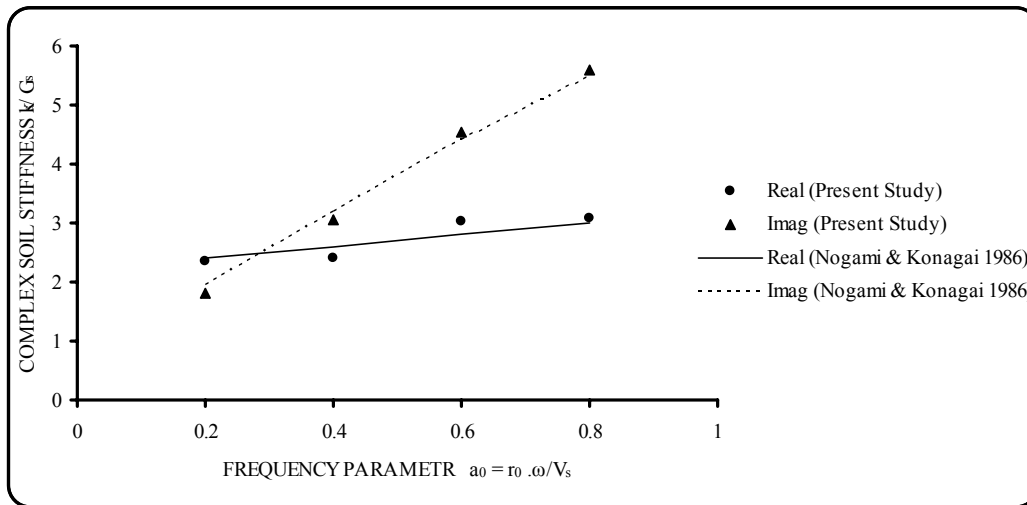


Fig. 3 Complex soil stiffness versus frequency: comparison of present study with Nogami and Konagai (1986)

2. Verification for Pile-Head Stiffness

Figure 4 shows the relationship between the dimensionless pile-head stiffness and dimensionless frequency due to the application of axial load. In this case also, trends of results are similar to those presented by Nogami and Konagai (1986). However, the imaginary part of the pile-head stiffness shown by the present study is significantly greater than that presented by Nogami and Konagai (1986), which may be attributed to the fact that slenderness ratio of the pile is different in the two cases.

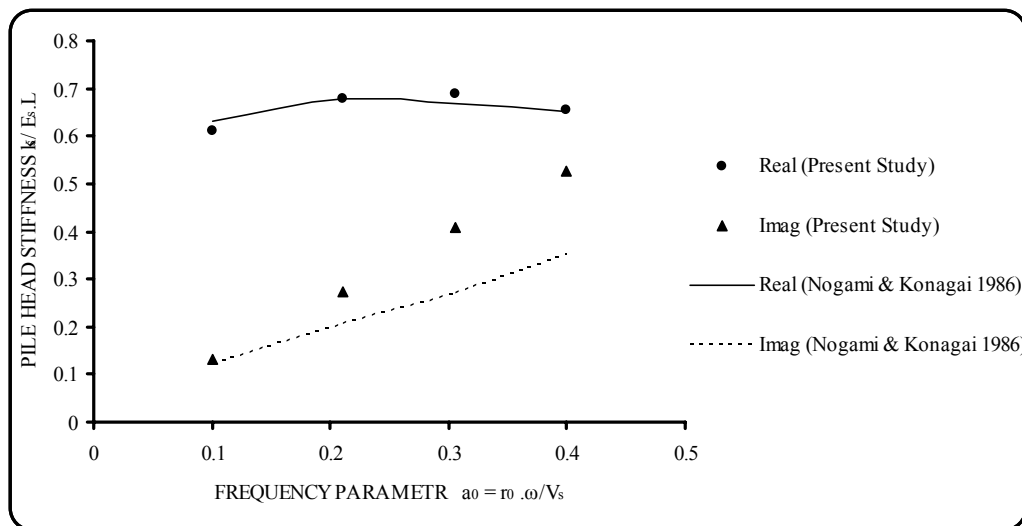


Fig. 4 Pile-head stiffness versus frequency: comparison of present study with Nogami and Konagai (1986)

3. Verification for Liquefaction Model

The result obtained from the liquefaction model is shown in Figure 5. It can be seen that the rate of generation of pore pressure first increases drastically and then decreases exponentially with number of cycles. Similar trend of results was shown by Gupta (1979).

DATA USED IN ANALYSIS

For the given soil profile, it is evaluated whether liquefaction will occur or not. First the zone of liquefaction is determined; for this purpose, the input data used in the analysis is shown in Table 1. A homogeneous soil stratum of 20 m depth is considered to be resting on the bedrock.

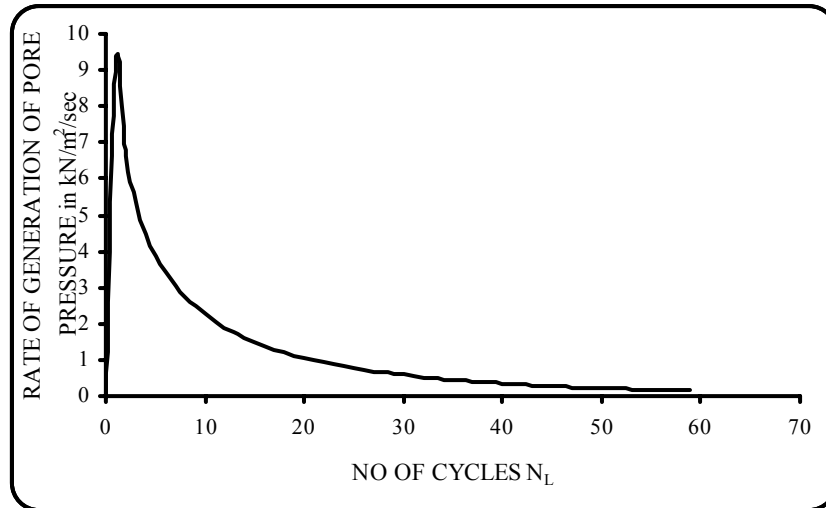


Fig. 5 Rate of generation of pore pressure versus number of cycles

Table 1: Input Data Used to Find the Zone of Liquefaction

Input Data	Value
PGA (a_{max})	0.16g
Magnitude of the earthquake (M)	7.5
Equivalent Number of Cycles (N_{eq}) for $M = 7.5$	20
D_{50} of sand	0.2 mm
Relative density (D_r)	40%
Thickness of soil stratum	20.0 m
Saturated mass density of soil (ρ_{sat})	$1.804 \times 10^3 \text{ kg/m}^3$

Zone of Liquefaction: Figure 6 shows a comparison of two sets of results, i.e., average shear stress τ_{av} versus depth (using Equation (1)) and shear stress causing liquefaction, τ , versus depth (using Equation (2)). It can be observed that for PGA equal to 0.16g and for earthquake of magnitude 7.5, soil stratum will liquefy for the whole depth. Here the position of water table is assumed at the ground surface itself. At higher depths, there is a wide margin between the two curves (see Figure 6), which may be attributed to the fact that relative density of the soil stratum is only 40% (for loose soil) and, therefore, it will be subjected to severe liquefaction.

RESULTS AND DISCUSSION

The behavior of soil-pile interaction is investigated in the following sections with respect to the variations in frequency of excitation and pile diameter. Effects of these parameters on the maximum displacement and interacting forces are evaluated considering liquefaction.

For the parametric study, the data used is shown in Table 2.

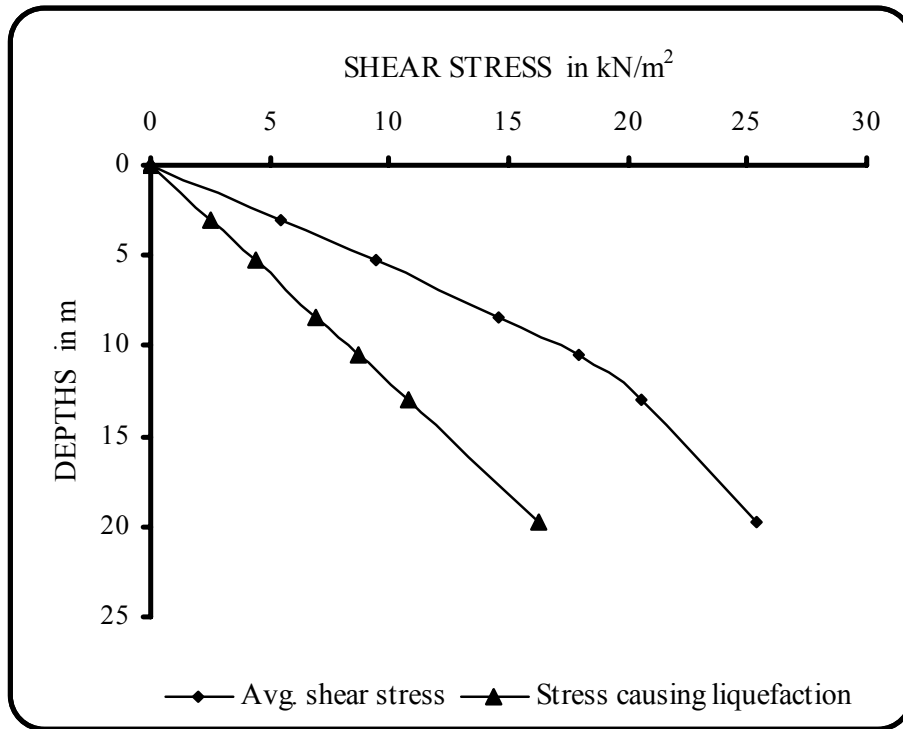


Fig. 6 Zone of liquefaction

Table 2: Input Data Used in the Parametric Study

Input Data	Value
Amplitude of harmonic force excitation (P)	100 kN
Dimensionless frequency of excitation (a_0)	0.1, 0.2, 0.3, 0.4
Pile diameter ($2r_0$)	1.0 m
Length of the pile	20.0 m
Modulus of elasticity of the pile (E_p)	25.00×10^9 N/m ²
Shear modulus of the soil (G_s)	71.77×10^6 N/m ²
Shear wave velocity (V_s)	199.46 m/s
Poisson's ratio of the soil (ν)	0.40

1. Effects of Frequency

Axial displacements due to the pile-soil interaction for different values of dimensionless frequency a_0 without and with liquefaction are compared in Figures 7(a) and 7(b), respectively.

In Figures 7(a) and 7(b), it may be observed that displacements at lower frequencies are more than those at the higher frequencies. This is because the dimensionless fundamental natural frequency a_0 of the soil is very low and close to the lowest frequency considered ($= 0.1$), with a_0 calculated as follows: $a_0 = \omega r_0 / V_s = 2\pi \times f_0 \times r_0 / V_s = 2\pi \times V_s \times r_0 / V_s \times 4h = \pi \times r_0 / 2h \approx 0.04$. Also for all frequencies, the maximum displacement is observed at the ground surface, which may be attributed to higher interacting

forces near the pile head. Also the effect of frequencies is diminishing at the higher values of a_0 . The overall trend of the results is similar for both non-liquefied and liquefied cases.

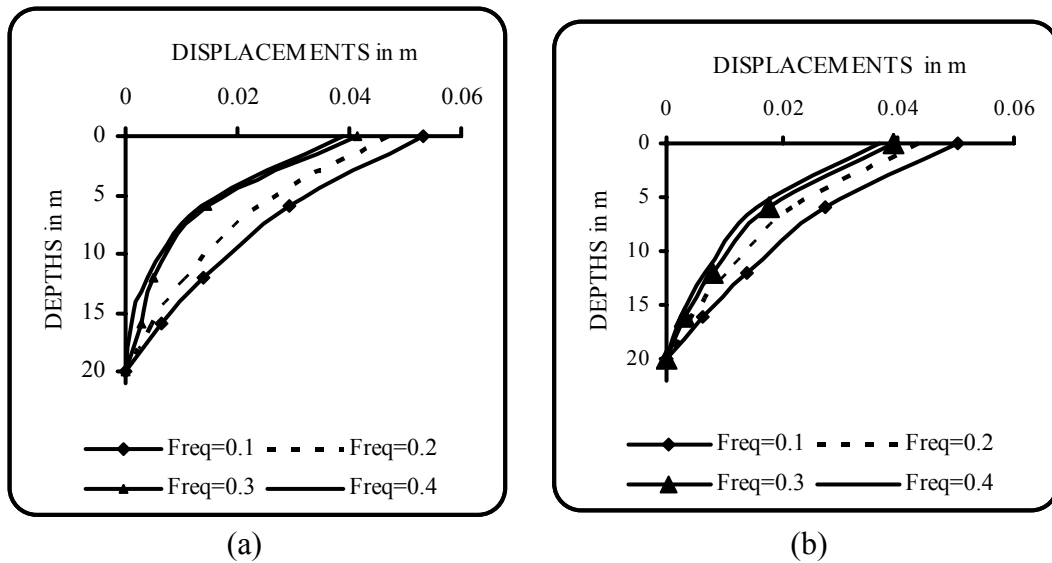


Fig. 7 Comparison of the axial displacements at different values of dimensionless frequency a_0 for the (a) non-liquefied and (b) liquefied cases

Interacting forces due to the pile-soil interaction (without and with liquefaction) for different frequencies are compared in Figures 8(a) and 8(b), respectively. The interacting forces increase with the frequency of excitation, when liquefaction is not considered. However, for the liquefied soil, the effect of frequency is not significant and peak value (at the ground surface) is lower than that in the non-liquefied case. Further, for the liquefied soil, it appears that the effect of liquefaction dominates over the frequency of excitation.

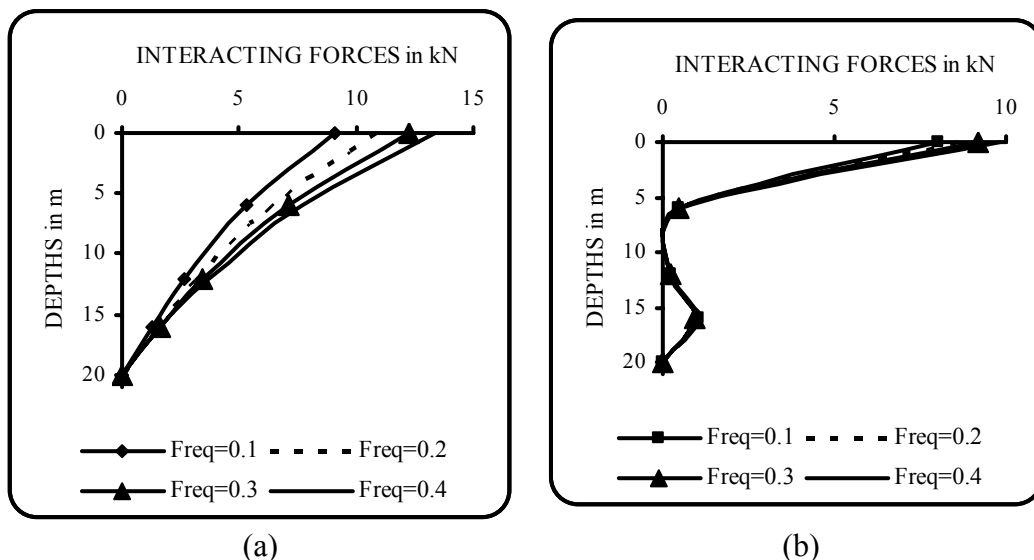


Fig. 8 Comparison of the interacting forces for different values of dimensionless frequency a_0 for the (a) non-liquefied and (b) liquefied cases

2. Effects of Liquefaction

Axial displacements for the non-liquefaction (NL) and liquefaction (L) conditions are compared in Figures 9(a) and 9(b) for the dimensionless frequencies equal to 0.3 and 0.4, respectively. The axial displacements at higher depths with liquefaction are greater than those without liquefaction. This is

because of the degradation of soil due to liquefaction. The percentage increase in the displacements due to liquefaction is observed as follows. For $a_0 = 0.3$, the percentage increase in the displacement is 22.76% and 36.3% at the depths of 6 and 12 m, respectively. Similarly for $a_0 = 0.4$, this increase is 12.9% and 42.6% at the depths of 6 and 12 m, respectively. Thus due to the effects of liquefaction, displacements are increased significantly.

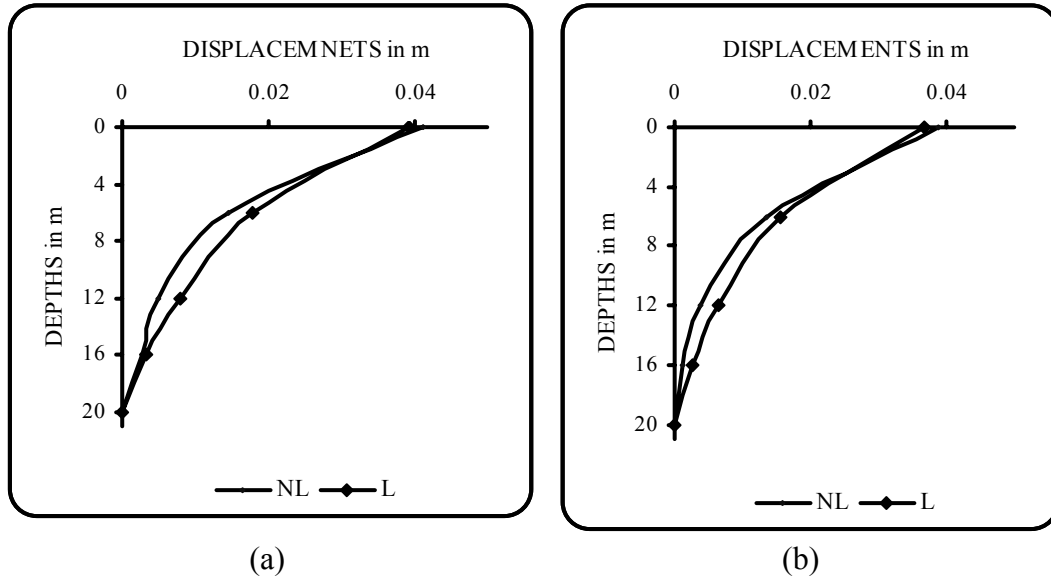


Fig. 9 Effects of liquefaction on axial displacements for two different frequencies: (a) $a_0 = 0.3$, and (b) $a_0 = 0.4$

Figures 10(a) and 10(b) show the effects of liquefaction on the interacting forces for $a_0 = 0.3$ and 0.4, respectively. It can be observed that due to liquefaction, the interacting force is drastically reduced. It is because of the reduction in the shear strength of soil due to liquefaction that lower interacting forces are obtained.

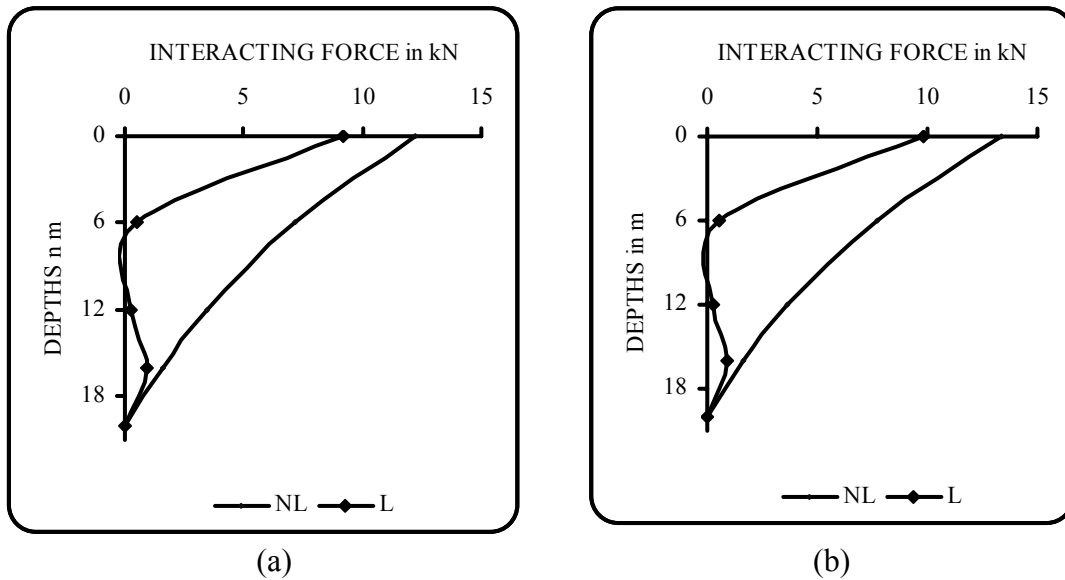


Fig. 10 Effects of liquefaction on interacting forces for two different frequencies: (a) $a_0 = 0.3$, and (b) $a_0 = 0.4$

3. Effects of Pile Diameter

The effects of variation in geometric properties are considered by changing the diameter of the pile for the liquefiable soil. The diameters of the pile considered are $d = 1$ and 0.5 m. The results are shown in Figures 11(a) and 11(b) for $a_0 = 0.3$ and 0.4 , respectively. For both frequencies, it can be observed that the displacements are considerably higher for the smaller diameter pile. This is as expected because decreasing the cross-sectional area would increase the stresses and thus the interaction forces; this, in turn, will increase the displacements. Thus a smaller diameter pile may be vulnerable to large displacements and also to instability failure in axial vibration (Bhattacharya et al., 2004).

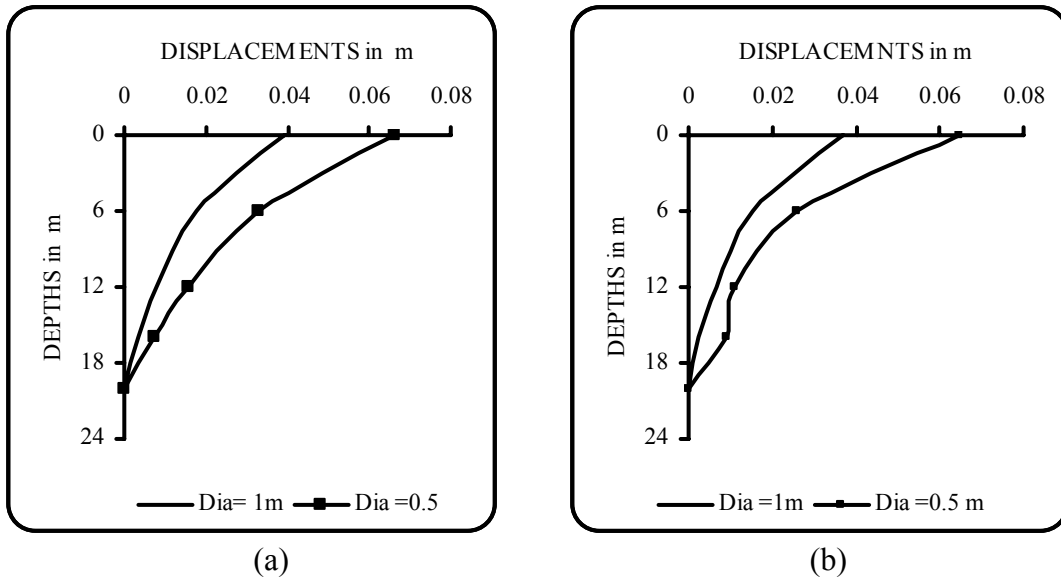


Fig. 11 Effects of pile diameter on axial displacements for two different frequencies (in liquefiable soil): (a) $a_0 = 0.3$, and (b) $a_0 = 0.4$

CONCLUSIONS

The following conclusions may be derived from this study:

1. The axial displacements developed due to the pile-soil interaction for different frequencies without and with liquefaction are significant near the natural frequency of the soil stratum.
2. Due to liquefaction, displacements are increased significantly while interaction forces decrease drastically.
3. Effect of frequency on both displacements and interaction forces is relatively small for liquefiable soils. It appears that the effect of liquefaction dominates over that of frequency.
4. In liquefiable soils, the displacements for small-diameter piles are considerably greater than those for the large-diameter piles.

In the present analysis, liquefaction has been considered along with the soil-pile interaction for axial vibration. This research work has wide practical applications in analyzing and designing pile foundations passing through liquefiable soil layers.

Here for simplicity, a simple visco-elastic soil model (i.e., Winkler soil model) has been considered in the analysis. However, the liquefaction being a nonlinear problem, an advanced constitutive model of soil with yielding of material may be considered. The results presented may differ in the case of the advanced soil model; nonetheless the paper demonstrates qualitatively the effects of liquefaction on soil-pile interaction in axial vibration.

REFERENCES

1. Bhattacharya, S., Madabhushi, S.P.G. and Bolton, M.D. (2004). “An Alternative Mechanism of Pile Failure in Liquefiable Deposits during Earthquakes”, *Geotechnique*, Vol. 54, No. 3, pp. 203–213.

2. El Naggar, M.H. and Novak, M. (1994). "Nonlinear Model for Dynamic Axial Pile Response", *Journal of Geotechnical Engineering*, ASCE, Vol. 120, No. 2, pp. 308–329.
3. Finn, W.D.L. and Fujita, N. (2002). "Piles in Liquefiable Soils: Seismic Analysis and Design Issues", *Soil Dynamics and Earthquake Engineering*, Vol. 22, No. 9–12, pp. 731–742.
4. Gupta, M.K. (1979). "Liquefaction of Sand during Earthquake", Ph.D. Dissertation, Department of Earthquake Engineering, University of Roorkee, Roorkee.
5. Katsuichiro, H., Tomoaki, I., Hideo, T., Kohji, K., Yuji, M., Osamu, K. and Robert, N. (2004). "Experimental Study on Soil-Pile-Structure Interaction in Liquefiable Sand Subjected to Blast-Induced Ground Motion", *Proceedings of the 13th World Conference on Earthquake Engineering*, Vancouver, Canada, Paper No. 190 (on CD).
6. Konagai, K. and Nogami, T. (1987). "Time Domain Axial Response of Dynamically Loaded Pile Groups", *Journal of Engineering Mechanics*, ASCE, Vol. 113, No. 3, pp. 417–430.
7. Liyanapathirana, D.S. and Poulos, H.G. (2002a). "Numerical Simulation of Soil Liquefaction due to Earthquake Loading", *Soil Dynamics and Earthquake Engineering*, Vol. 22, No. 7, pp. 511–523.
8. Liyanapathirana, D.S. and Poulos, H.G. (2002b). "A Numerical Model for Dynamic Soil Liquefaction Analysis", *Soil Dynamics and Earthquake Engineering*, Vol. 22, No. 9–12, pp. 1007–1015.
9. Liyanapathirana, D.S. and Poulos, H.G. (2005). "Pseudostatic Approach for Seismic Analysis of Piles in Liquefying Soil", *Journal of Geotechnical and Geoenvironmental Engineering*, ASCE, Vol. 131, No. 12, pp. 1480–1487.
10. Maheshwari, B.K., Truman, K.Z., Gould, P.L. and El Naggar, M.H. (2005). "Three-Dimensional Nonlinear Seismic Analysis of Single Piles Using Finite Element Model: Effects of Plasticity of Soil", *International Journal of Geomechanics*, ASCE, Vol. 5, No. 1, pp. 35–44.
11. Martin, G.R., Seed, H.B. and Finn, W.D.L (1975). "Fundamentals of Liquefaction under Cyclic Loading", *Journal of the Geotechnical Engineering Division*, *Proceedings of ASCE*, Vol. 101, No. GT5, pp. 423–438.
12. Martin, P.P. and Seed, H.B. (1979). "Simplified Procedure for Effective Stress Analysis of Ground Response", *Journal of the Geotechnical Engineering Division*, *Proceedings of ASCE*, Vol. 105, No. GT6, pp. 739–758.
13. Miwa, S., Ikeda, T. and Sato, T. (2006). "Damage Process of Pile Foundation in Liquefied Ground during Strong Ground Motion", *Soil Dynamics and Earthquake Engineering*, Vol. 26, No. 2–4, pp. 325–336.
14. Nath, U.K. (2006). "Pile-Soil Interaction in Liquefiable Soils", M.Tech. Thesis, Department of Civil Engineering, Indian Institute of Technology Roorkee, Roorkee.
15. Nogami, T. and Konagai, K. (1986). "Time Domain Axial Response of Dynamically Loaded Single Piles", *Journal of Engineering Mechanics*, ASCE, Vol. 112, No. 11, pp. 1241–1252.
16. Novak, M. (1974). "Dynamic Stiffness and Damping of Piles", *Canadian Geotechnical Journal*, Vol. 11, No. 4, pp. 574–598.
17. Novak, M., Nogami, T. and Aboul-Ella, F. (1978). "Dynamic Soil Reaction for Plane Strain Case", *Journal of the Engineering Mechanics Division*, *Proceedings of ASCE*, Vol. 104, No. EM4, pp. 953–959.
18. Prakash, S. (1981). "Soil Dynamics", McGraw-Hill Book Company, New York, U.S.A.
19. Seed, H.B. and Idriss, I.M. (1971). "Simplified Procedure for Evaluating Soil Liquefaction Potential", *Journal of the Soil Mechanics and Foundations Division*, *Proceedings of ASCE*, Vol. 97, No. SM9, pp. 1249–1273.
20. Seed, H.B., Martin, P.P. and Lysmer, J. (1976). "Pore-Water Pressure Changes during Soil Liquefaction", *Journal of the Geotechnical Engineering Division*, *Proceedings of ASCE*, Vol. 102, No. GT4, pp. 323–346.
21. Wilson, D.W. (1998). "Soil-Pile-Superstructure Interaction in Liquefying Sand and Soft Clay", Report UCD/CGM-98/04, Department of Civil & Environmental Engineering, University of California, Davis, U.S.A.

28th ISET Annual Lecture

**FOUNDATIONS FOR INDUSTRIAL MACHINES AND
EARTHQUAKE EFFECTS**

K.G. Bhatia

Center for Applied Dynamics
D-CAD Technologies, New Delhi

ABSTRACT

Improvement in manufacturing technology has provided machines of higher ratings with better tolerances and controlled behaviour. These machines give rise to considerably higher dynamic forces and thereby higher stresses and, in return, demand improved performance and safety leaving no room for failures. This paper highlights need for a better interaction between foundation designer and machine manufacturer to ensure improved machine performance. The paper also describes the design aids/methodologies for foundation design. Various issues related to mathematical modeling and interpretations of results are discussed at length. Intricacies of designing vibration isolation system for heavy-duty machines are also discussed. Influences of dynamic characteristics of foundation elements, viz., beams, columns, and pedestals etc. on the response of machine, along with some case studies, are also presented. The paper also touches upon the effects of earthquakes on machines as well as on their foundations. Use of commercially available finite element packages, for analysis and design of the foundation, is strongly recommended, but with caution.

KEYWORDS: Machine Foundation, Dynamic Response, Seismic Qualification, Design Aids, Vibration Isolation

INTRODUCTION

The dynamics of machine-foundation system is an involved task in itself and consideration of earthquake effects further adds to its complexity. The performance, safety and stability of machines depend largely on their design, manufacturing and interaction with environment. In principle machine foundations should be designed such that the dynamic forces of machines are transmitted to the soil through the foundation in such a way that all kinds of harmful effects are eliminated (Barkan, 1962; Bhatia, 1984, 2006, 2008; Major, 1980; Prakash and Puri, 1988; Srinivasulu and Vaidyanathan, 1980). In the past, simple methods of calculation were used, most often involving the multiplication of static loads by an estimated dynamic factor and the result being treated as an increased static load without any knowledge of the actual safety factor. Because of this uncertainty, the value of the adopted dynamic factor was usually too high, although practice showed that during operation harmful deformations did result in spite of using such excessive factors. This necessitated a deeper scientific investigation of dynamic loading. A more detailed study became urgent because of the development of machines of higher capacities (Bhatia, 1984).

Machines of higher ratings gave rise to considerably higher stresses thereby posing problems with respect to performance and safety. This called for development partly in the field of vibration technique and partly in that of soil mechanics. Hence new theoretical procedures were developed for calculating the dynamic response of foundations (Bhatia, 2006).

Based on the scientific investigations carried out in the last few decades it has been established that it is not enough to base the design only on the vertical loads multiplied by a dynamic factor, even if this factor introduces a dynamic load many times greater than the original one. It should be remembered that operation of the machines generates not only vertical forces, but also forces acting perpendicular to the axis; it is thus not enough to take into account the vertical loads only and to multiply those by a selected dynamic factor (Bhatia, 2006, 2008). It has also been found that the suitability of machine foundations depends not only on the forces to which they will be subjected to, but also on their behaviour, when

exposed to dynamic loads, which depends on the speed of the machine and natural frequency of the foundation. Thus a vibration analysis becomes necessary. Each and every machine foundation does require detailed vibration analysis providing insight into the dynamic behaviour of foundation and its components for satisfactory performance of the machine. The complete knowledge of load-transfer mechanism from the machine to the foundation and also the complete knowledge of excitation forces and associated frequencies are a must for the correct evaluation of machine performance.

All machine foundations, irrespective of the size and type of machine, should be regarded as engineering problems and their designs should be based on sound engineering practices. Dynamic loads from the machines causing vibrations must be duly accounted for to provide a solution, which is technically sound and economical. Though advanced computational tools are available for precise evaluation of dynamic characteristics of machine-foundation systems, their use in design offices, which was limited in the past, has now been found to be quite common. A machine-foundation system can be modeled either as a two-dimensional structure or as a three-dimensional structure.

For mathematical modeling and analysis, valid assumptions are made keeping in view the following:

- The mathematical model should be compatible with the prototype structure within a reasonable degree of accuracy.
- The mathematical model has to be such that it can be analysed with the available mathematical tools.
- The influence of each assumption should be quantitatively known with regard to the response of the foundation.

Vibration isolation techniques have also been used to reduce vibrations in the machines. Isolation leads to reduction in the transmissibility of the exciting forces from the machine to the foundation and vice-versa. Use of vibration isolation devices is one of the methods by which one can achieve satisfactory performance, which in turn can result in minimizing failures and reduce downtime on account of high vibrations. However, for equipment on elevated foundations, it is desirable to have support structure stiffness sufficiently higher than the overall stiffness of isolation system in order to get the desired isolation efficiency (Bhatia, 2008). The support structure, a 3-D elevated structural system, possesses many natural frequencies. The vibration isolation system, comprising the machine, inertia block and the isolation devices, also has six modes of vibration having specific stiffness values corresponding to each mode of vibration. It is of interest to note that the lateral stiffness of an elevated structure is very much lower than its vertical stiffness. If this lower (lateral) stiffness is comparable to the stiffness of isolators, it certainly affects the overall stiffness and thereby the response of the machine-foundation system. Hence, the lateral stiffness of the support structure must also be computed and considered while selecting the isolators. Finally it may be desirable to carry out detailed dynamic analysis of the complete system including the substructure.

MACHINE-FOUNDATION SYSTEM

The main constituents of a typical machine-foundation system are

- machine: rotary machines, reciprocating machines, impact machines;
- foundation: block foundations, or frame foundations; and
- support medium: soil continuum, or a soil-pile system, or a substructure that, in turn, is supported over the soil continuum or soil-pile system.

Dynamic forces are (i) internally generated forces by the machine itself, or (ii) externally applied forces (that are applied directly to the machine, or transmitted through the support medium/foundation).

Figure 1 shows the schematic of dynamics between various elements of a machine-foundation system. It is seen that all the three constituents of the machine-foundation system, viz., machine, foundation and soil, contribute to the frequency of the system. This system, when subjected to dynamic forces (whether internally generated, externally applied, or transmitted through the soil), results in response of the system.

MODELING AND ANALYSIS

Every foundation designer should remember that he/she is dealing with machines weighing several tonnes and is required to design the foundations having dimensions of several meters but with amplitudes restricted to only a few microns. The designer, therefore, must clearly understand the assumptions,

approximations, and simplifications made during the modeling and must recognize their influence on the response. It is this aspect that makes modeling and analysis a very important part of design.

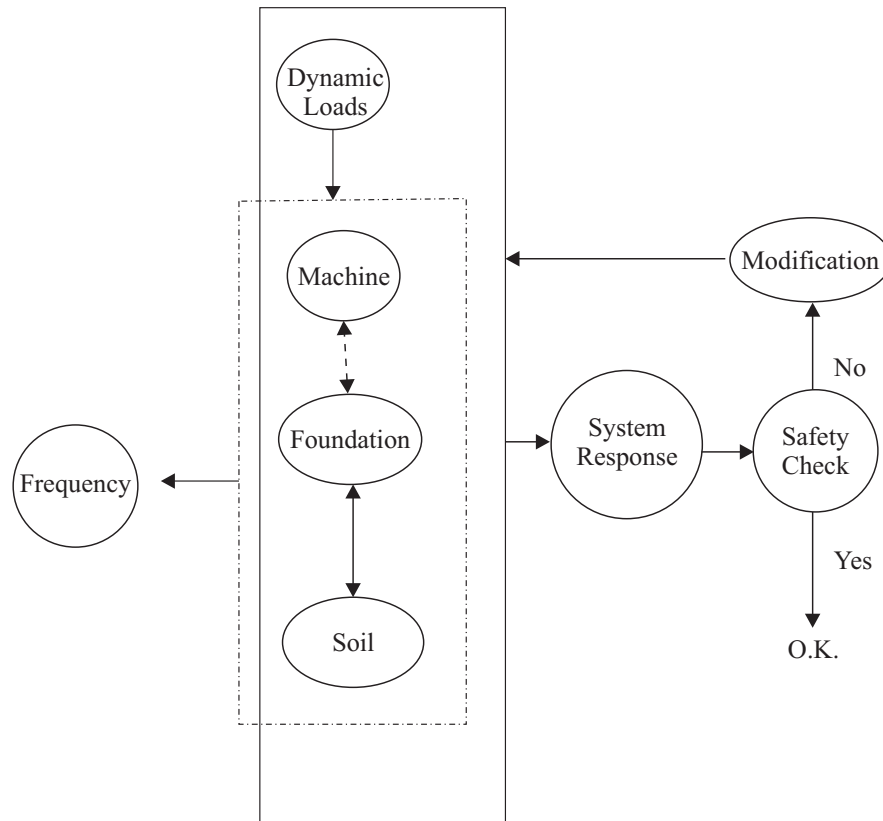


Fig. 1 Schematic diagram of a machine-foundation system subjected to dynamic loads

For the purpose of analysis, the machine-foundation system is represented by an appropriate mathematical model with the basic objective that the model should be compatible with the prototype. For each mathematical representation, a host of assumptions and approximations are made. The extent of complexity introduced in the mathematical model directly influences the reliability of results. In addition, simplifications/approximations are also introduced to meet the limitations of the analytical tools. In other words, mathematical representation not only depends on the machine and foundation parameters but also depends on the analysis tools.

1. Manual Computational Method

1.1 Block Foundations

For the machines on block foundations, it is good enough to use simple formulations (which are equations of motion considering block as a rigid body supported on an elastic medium, i.e., soil). Whereas majority of the machine and foundation aspects are well taken care of by these procedures, there are some aspects, as given below, that cannot be fully managed by these manual computational methods.

1.2 Foundation Eccentricity

If foundation eccentricity is higher than the permissible value, the vertical mode of vibration will no longer remain uncoupled from the lateral and rotational modes (Barkan, 1962; Bhatia, 2008). It is undoubtedly easy to write equations of motion for such uncoupled modes, but getting closed-form solutions for those equations is not that simple, and computations may turn out to be complex. Further, getting transient response history may be a tedious task, though it is possible to evaluate transient response at any of the defined frequencies.

It is therefore recommended to use finite element (FE) analysis, wherever feasible, in order to include all these aspects. Further, this gives improved reliability on account of lesser number of

approximations/assumptions. This also permits visualization of animated mode shapes, and viewing of response amplitude build-up and stress concentration locations.

1.3 Frame Foundations

The formulations used for manual computations cover only standard/ideal frames, i.e., frame beam is rectangular in cross-section having machine mass at its center. Analysis of a single portal frame is based on the premise that longitudinal beams of a frame foundation are flexible enough to permit transverse frames to vibrate independently (Barkan, 1962; BIS, 1992). These procedures are only for very ideal cases, and most of the real-life machine foundations do not fall under this category. Some of the aspects that cannot be suitably accounted for by the manual computational methods (Bhatia, 2008; Ramdas et al., 1982) are

- haunches,
- machine mass at off-center locations of the beam,
- beams extended as cantilevers on one side/both sides of the frame beam,
- beams inclined in elevation supporting heavy machine mass,
- no frame beam at column locations,
- higher-order frame-column vibration frequencies,
- presence of solid thick deck within the frames, and
- depression/recess in the top deck.

Based on many design studies carried out by the author, it has been observed that

1. Variation in natural frequencies of a frame obtained manually compared to the FE method is of the order of 10% to 20% (Bhatia, 2008).
2. FE analysis confirms the presence of three-to-four additional frequencies between the first and second vertical modes as computed manually. These additional frequencies lie well within the operating range of the medium-RPM machines and may significantly contribute to the response.
3. In recognition of the higher reliability of the FE method, and the fact that manual computations give results that are in variance by 10% to 20% compared to the FE analysis, it has been suggested that no corrections need to be applied on account of either frame centerline dimensions or inclusion of haunches, etc.; all corrections put together will easily get absorbed by the available margins (Bhatia, 2008).

It is, therefore, recommended to use FE analysis with appropriate element types for the modeling of frame foundation. It is, however, recommended to use the manual analytical approach to evaluate free-vibration response for each frame to get a first-hand feeling of the frequency range of frames vis-à-vis the operating frequency and their sub- and super-harmonics.

2. Finite Element Method

Finite element method is the most commonly accepted analysis tool for the solution of engineering problems. Effective pre- and post-processing capabilities make modeling and interpretation of results simple. It is relatively easy to incorporate changes, if any, and to redo the analysis without much loss of time. Viewing of the animated mode shapes and dynamic response makes understanding of the dynamic behaviour of the machine foundation system relatively simpler. Design of machine foundation involves the consideration of machine, foundation and soil together as a system, subjected to applied or generated dynamic forces. Development of a specific FE-based package for the design of machine foundation is generally not feasible on account of (a) tight project schedules and (b) validation of results. Use of commercially available packages is more effective for design offices. There are many issues that need careful examination before finalizing the package, e.g., user friendliness, pre-processor capabilities (i.e., modeling capabilities), analysis capabilities, post-processor capabilities (related to the processing of results), etc., but the most important issue is the validation of results. Every package is a black box for the user and it has its associated limitations, some of which are explicit and some are implicit. Validation for some known sample cases, therefore, becomes a must before one accepts the results. The author has himself used many commercially available packages for the analysis and design of machine foundations during the course of his professional career. Finite element method enables the modeling of machine, foundation and soil in one go, which brings behaviour of the machine-foundation system closer to that of the prototype, resulting in improved reliability. Rigid-beam elements are used for modeling the machine whereas solid elements are used for modeling the foundation. In case soil is represented as continuum, it

is also modeled using the solid elements. In case soil is represented by equivalent springs, it could be modeled using spring elements or boundary elements. Modeling of each of the constituent is an art in itself and is briefly discussed below.

2.1 Machine

Machine is relatively rigid compared to the foundation and soil. It is considered contributing to the mass, only with its centre of gravity (CG) lying above the foundation level. While modeling the machine, the broad objective is to represent the machine in such a way that its mass is truly reflected, and CG of the overall mass of the model matches with that of the prototype. Thus, modeling of the machine with rigid links or rigid-beam elements is considered good enough. Machine mass is considered lumped at appropriate locations so as to correctly simulate the CG location. This should be cross-checked with the mass distribution given by the supplier/manufacturer.

Whether it is a block foundation or a frame foundation, lumping of the machine mass at the top level of the foundation is not desirable, as this will result in mismatch of the CG of the machine mass (in the vertical direction) of the model with that of the prototype. Figure 2(a) shows such a lumping for a typical block foundation (Bhatia, 2006, 2008). Such a representation does affect the mass moment of inertia and thereby the natural frequencies and the response. It is therefore essential that the CG of the machine mass in vertical direction must be matched with that of the prototype, as given by the manufacturer. Machine mass should be lumped at an appropriate level above the foundation, as shown in Figure 2(b). Similar concept should be used for modeling the bearing pedestals.

For advanced modeling, it is desirable to model the rotor and stator independently. The rotor is represented using a set of beam elements with corresponding section and material properties that represent the variation of rotor section along the machine axis, whereas the stator is modeled using the rigid links, with stator mass lumped at appropriate locations, such that the CG of mass matches with that provided by the supplier. Rotor support at the bearing locations should be modeled with the corresponding stiffness and damping properties offered by the bearings (Bhatia, 2008). Such a model is as shown in Figure 2(c). The bearing pedestals, however, are modeled as the rigid links.

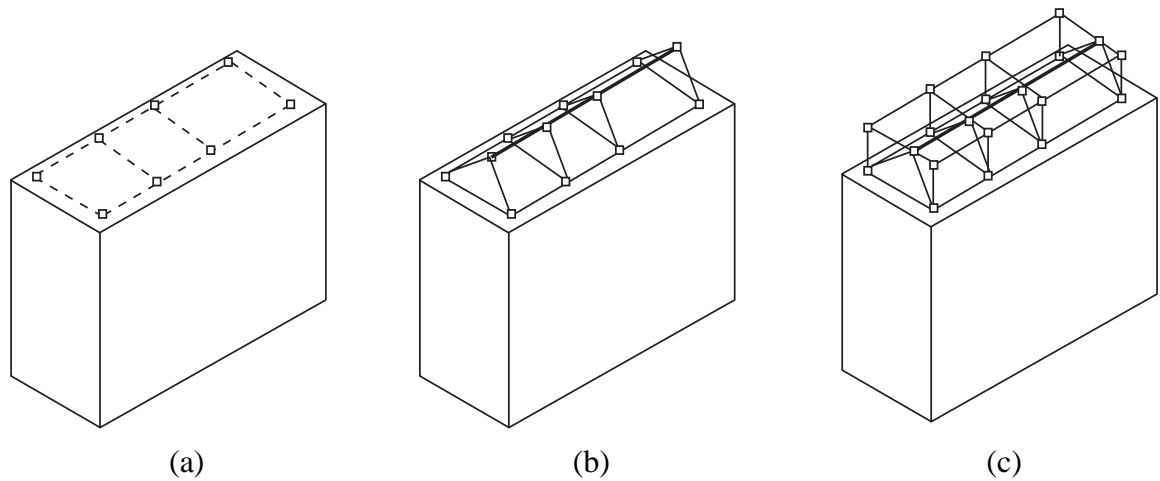


Fig. 2 Modeling of machine with foundation: (a) machine mass lumped at the foundation top, (b) machine masses lumped at the CG level of the machine, (c) rotor and stator modeled separately—masses lumped at the respective CG levels

2.2 Foundation

Block Foundation: A foundation block is a solid mass made of reinforced cement concrete (RCC) with required openings, depressions, raised pedestals, cutouts, bolt pockets, and extended cantilever projections. Solid elements are good enough for modeling a foundation block. A coarse mesh for the block and relatively finer mesh in the vicinity of openings, pockets, and cutouts is considered sufficient. Solid model and FE mesh of a typical foundation block are shown in Figure 3. Generally speaking, modeling the foundation block with 8-noded brick elements or 10-noded tetrahedral elements works reasonably well and is considered good enough. A higher order solid element would increase the size of

the model, requiring more computational time and power, while improvement in the results may only be marginal. Choice of element size is fairly subjective as it is problem-dependent. It is, therefore, not possible to specify firm guidelines regarding the choice of right element size that will be applicable to all types of problems. The judgment of optimum mesh density, however, would emerge after experience.

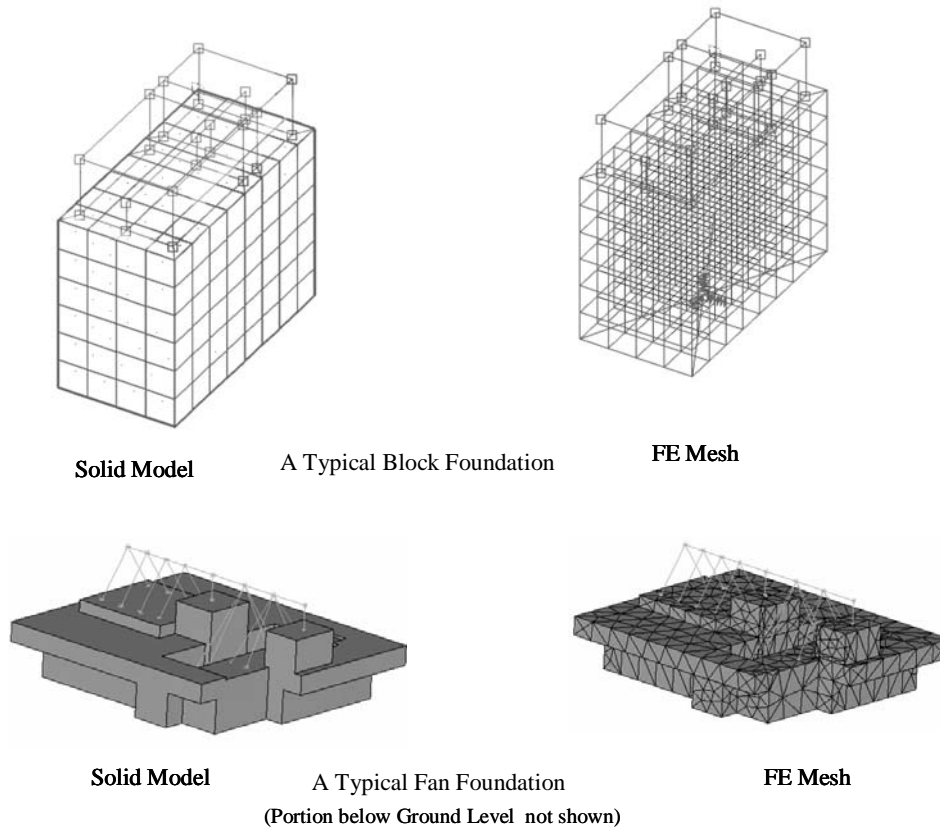


Fig. 3 Foundation block—solid model and FE mesh

Frame Foundation: A frame foundation comprises base raft, set of columns (which is equal to the number of frames), and top deck consisting of (longitudinal and transverse) beams and slabs. The top deck is made of RCC with required openings, depressions, raised pedestals, cutouts, bolt pockets and extended cantilever projections. In certain cases, haunches may also be provided between the columns and the top deck. There are many ways of representing the model of a frame foundation. One can model using the beam elements, shell elements, solid elements, or a combination of all of these. Models with the solid elements as well as beam and shell elements are shown in Figures 4(a) and 4(b) respectively. Each modeling style, however, will have associated limitations. For example, while modeling using the solid elements, one may not be able to get the bending moments and shear forces in the columns, beams and slabs, which are needed for the structural design of these members. When it is possible to get the bending moments and shear forces in the flexural members like beams, columns, slabs, etc., the modeling would not permit inclusion of the effects like haunches, depressions, cut-outs, raised blocks, projections, etc., as shown in Figure 4(c). It may be noted that a FE mesh of frame foundation with all the openings, pockets, cutouts, notches, etc., though feasible, is basically undesirable. It may unnecessarily add to the problem size and, thereby, to the computational time without any significant gain in the results. Only those elements that contribute significantly to the stiffness and mass, like large openings, sizeable depressions, etc., must be accounted for and modeled in detail, whereas the elements like pockets, small notches, etc. could easily be ignored while modeling. Since modeling of the top deck and base raft by the shell element is done at their mid-surface locations, it usually results in increased column heights, thus making the system more flexible than the prototype. Necessary modifications therefore are necessary to overcome this deficiency. Similar is the case while modeling the machine. Use of the rigid links is recommended to cover up such deficiencies. Here again, a coarse mesh for the foundation in general, and relatively finer mesh in the vicinity of openings, depressions, raised pedestals, pockets, and cutouts is considered adequate. The judgment of optimum mesh density, however, would emerge only after experience.

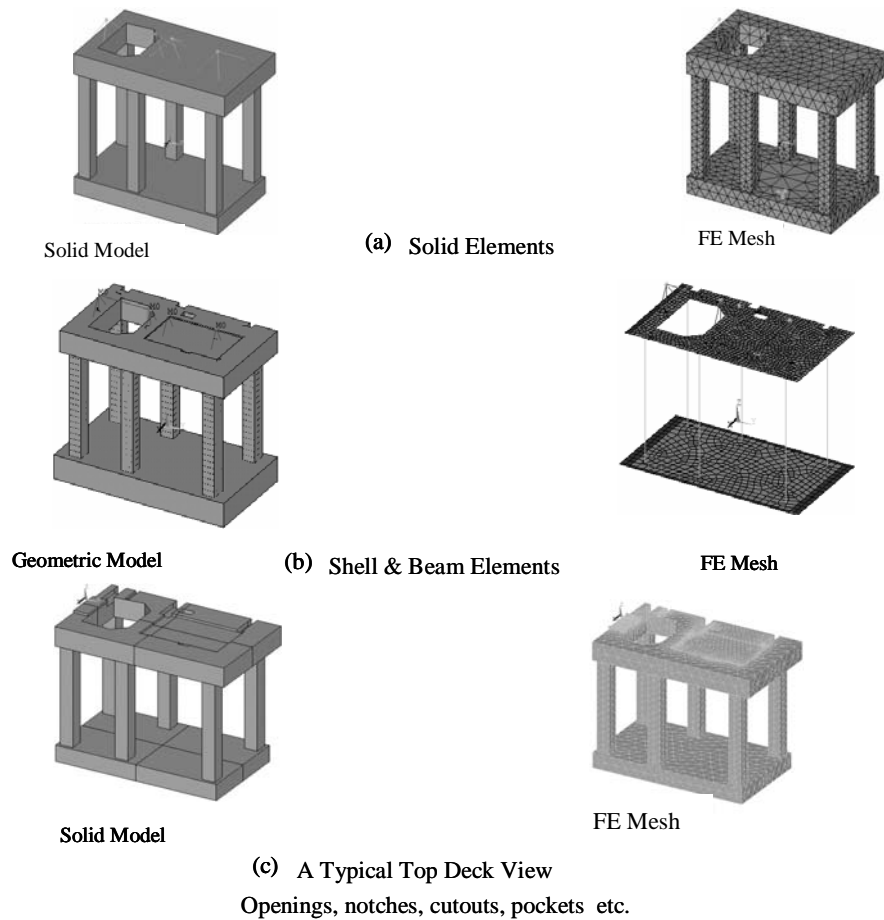


Fig. 4 Frame foundation—solid element model and shell-beam model

2.3 Soil

2.3.1 Soil Modeling

Use of the FE analysis has become the state of art for the design of machine foundations. There are many ways of mathematical representation of the soil. We limit our discussion here only to two ways that are common in the design office practices for the FE analysis and design of foundations.

Soil Represented by a Set of Equivalent Springs: Two types of representations are commonly used in the FE modeling of the foundation:

- a) The soil is represented by a set of three translational springs and three rotational springs, attached at the CG of the base, as shown in Figure 5(a). This kind of representation yields results (i.e., frequencies and amplitudes) that are found to be in close agreement with the manual computations (Barkan, 1962; Bhatia, 1981, 2006, 2008; Prakash and Puri, 1988).
- b) The soil is represented by a set of three translational springs, attached at each node at the base of the foundation in contact with the soil, as shown in Figure 5(b). This kind of representation provides an upper bound to the overall rotational stiffness offered by the soil about the X-, Y-, and Z-axes (Bhatia, 2008).

Soil Represented as Continuum: Soil domain in true sense is an infinite domain, and for analysis purposes, it becomes necessary to confine it to a finite domain when soil is considered as continuum (Bhatia, 2008; Prakash, 1981). The broad issues that need to be addressed are

- a) the extent of the soil domain to be considered for the modeling; and
- b) whether to consider soil domain only below the foundation base (in which case the foundation is not embedded) or to consider the foundation embedded into the soil domain.

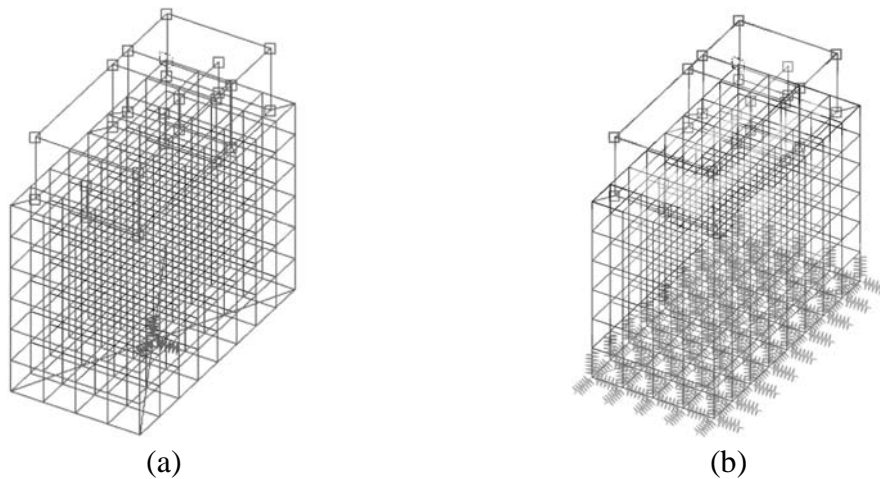


Fig. 5 Various methods of soil representation for FE modeling: (a) soil represented by a set of three translational springs, k_x , k_y , k_z , and three rotational springs, k_θ , k_ψ , k_ϕ , applied at the CG of the base of the foundation; (b) soil represented by a set of three translational springs, k_x , k_y , k_z , applied at each node in contact with the soil at the foundation base

2.3.2 Extent of Soil Domain

For FE modeling, it is well known that a narrow domain with fixed boundaries is not likely to represent a realistic soil behaviour, whereas a very large domain would result in an increased problem size. It is, therefore, necessary to find an optimum value that reflects the realistic behaviour of soil without significant loss in accuracy. Different designers adopt their own practices based on the rule of thumb, while deciding on the extent of soil domain to be modeled with the foundation. The extent of soil domain has been found to vary from three to eight times the width of the foundation, to be provided on all the five sides of the foundation. It is to be noted that such a consideration is good enough for academic purposes only. In a real industrial situation, no foundation could remain isolated from other equipment/structure foundations within this finite soil domain. In other words, many other equipment/structure foundations would exist within the range of three to eight times the dimension of the foundation in each X-, Y-, and Z-direction. Thus, in the author's opinion, the computed behaviour of a foundation as a stand-alone foundation is likely to differ with the actual one. It is also true that the modeling of all the equipment and structure foundations of a project in one single go is neither feasible nor necessary (Bhatia, 2008). Here too, a mesh consisting of the solid elements is good enough. As the soil domain is very large compared to the foundation, a relatively coarser mesh of the soil is considered to be adequate. Refinement of the mesh size may be adopted, if considered necessary, for specific cases. The choice of element size remains subjective.

The precise decision on the extent of soil domain still remains a question mark. Even the academicians have provided no definite answer to this issue. It is also true that a practicing engineer, in view of his/her tight time schedule, can neither afford to search for the optimum domain size nor ignore the problem. In the author's considered opinion, soil domain equal to three to five times the lateral dimensions in plan on either side of the foundation and five times along the depth should work out to be reasonably good. The finite soil domain is modeled along with the foundation block using the FE idealization. Appropriate soil properties in terms of the elastic modulus/shear modulus and Poisson's ratio are assigned to the soil. If the soil profile indicates the presence of layered media, appropriate soil properties are assigned to the respective soil layers, with variation in soil properties along the length, width, and depth of the soil domain.

2.3.3 Unembedded and Embedded Foundations

While modeling soil along with the foundation, two cases arise:

- i) Soil domain is modeled below the foundation up to three to five times the width of the foundation along the length, breadth, and depth of the foundation. This makes the foundation not embedded into the soil, as shown in Figure 6(a).

- ii) Soil domain is modeled right from the ground level encompassing the foundation up to three to five times the width of the foundation along the length, breadth, and depth of the foundation. This makes the foundation embedded into the soil, which is a realistic situation. This representation is shown in Figure 6(b).

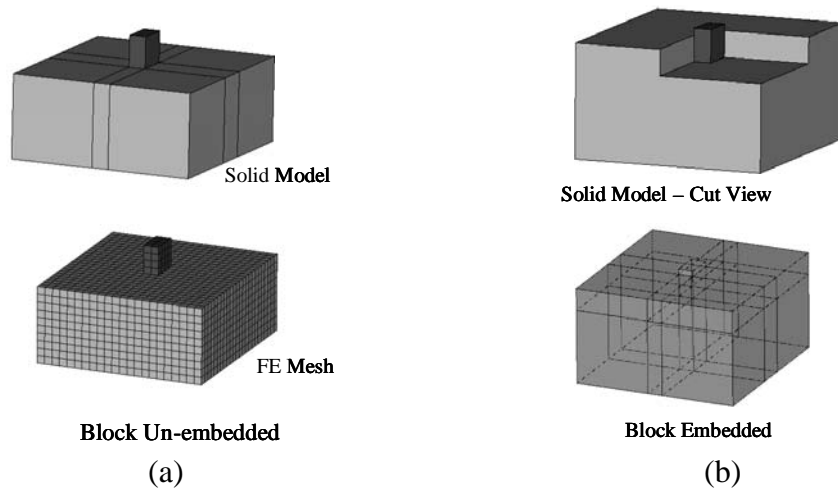


Fig. 6 Various methods of soil representation for FE modeling: (a) soil represented by a continuum below the foundation base, extending three times the width of the foundation along the length and the width and five times the depth of the foundation along the depth; (b) soil represented by a continuum starting from the ground level, extending three times the width of the foundation along the length and the width and five times the depth of the foundation along the depth

To investigate as to how each method of soil representation compares with others, free-vibration analysis of a typical block foundation is performed using each method of soil representation having same/compatible soil properties (Bhatia, 2008):

- Case-1: The soil is represented by a set of six springs attached at the CG of the base of the foundation.
- Case-2: The soil is represented by a set of three springs attached at each node in contact with the soil at the base of the foundation. In total 45 nodes are considered in contact with the soil. Translational stiffness at each node is therefore $1/45$ of k_x, k_y, k_z as given above.
- Case-3: The soil is represented as continuum below the foundation base level, i.e., the foundation is not embedded. The soil domain considered is 10 m on all the five sides of the foundation.
- Case-4: The soil is represented as continuum right from the ground level all around the foundation, i.e., the foundation is embedded. Here again, the soil domain considered is 10 m on all the four sides (in plan) of the foundation. The ground level is considered at 0.75 m below the top of the block. The soil domain along depth is taken as $(10 + 3 =) 13$ m from the ground level.

The data considered is as under:

- foundation block dimensions (along the Z-, X-, Y-axes): $4 \times 2 \times 3.75$ m;
- coefficient of uniform compression: $C_u = 4.48 \times 10^4$ kN/m³;
- soil spring stiffness (translational): $k_y = 35.84 \times 10^4$ kN/m, $k_x = k_z = 17.97 \times 10^4$ kN/m;
- soil spring stiffness (rotational): $k_\phi = 95.5 \times 10^4$ kN-m/rad (about the X-axis), $k_\psi = 44.8 \times 10^4$ kN-m/rad (about the Y-axis), $k_\theta = 23.9 \times 10^4$ kN-m/rad (about the Z-axis);
- $\rho_{\text{soil}} = 1.8$ t/m³, $\nu_{\text{soil}} = 0.33$, $E_{\text{soil}} = 89,218$ kN/m²; and
- $\rho_{\text{conc}} = 2.5$ t/m³; $\nu_{\text{conc}} = 0.15$; $E_{\text{conc}} = 2 \times 10^7$ kN/m².

Modal frequencies are listed in Table 1. The comparison reveals interesting observations as follows:

- a) The translational mode frequencies for Case-3 and Case-4, i.e., when soil is considered as continuum, are much lower than those obtained for Case-1 and Case-2.

- b) Discrepancies in rotational frequencies of Case-3 and Case-4 are also significant in comparison with those of Case-1 and Case-2.
- c) For Case-2, both linear as well as rotational frequencies are marginally lower than those for Case-1. For block foundations, since soil flexibility is a controlling parameter that governs the response of the foundation, the author recommends only the use of modeling as in Case-1 and Case-2. In view of the above observations, modeling of soil as continuum is not recommended for the block foundations. Designers, however, may take their own need-based decisions.

Table 1: Modal Frequencies (in Hz)

	Soil Representation Type	Predominant Mode Direction					
		X	Y	Z	Θ_x	Θ_y	Θ_z
1	Soil represented by six springs (three linear and three rotational) at the CG of the foundation base	15.4	10.9	15	5.6	9.4	3.62
2	Soil represented by three equivalent linear springs at the foundation base at each node in contact with the soil	15.2	11	14	4.9	8.9	3.24
3	Soil continuum—foundation considered as not embedded	5.16	6.8	6.1	7	7.6	6.97
4	Soil continuum—foundation considered as embedded	6.52	5.96	6.3	7	7.3	7.23

Whichever modeling criteria are finally chosen by the designer, it is strongly recommended that validation of the FE results with the manual computations must be done for very simple problems using the same modeling criteria, before those are adopted for the actual design. Such a caution is essential as one often tends to feel that whatever results are obtained by using a computer code are bound to be correct.

PARAMETERS INFLUENCING VIBRATION

Foundation parameters that influence the vibrations of a machine-foundation system are mainly (i) overall foundation size, (ii) depth of embedment, (iii) sizes of the foundation members like columns, beam, deck slab, cantilever projections, etc., (iv) dynamic soil parameters or dynamic soil-pile properties, and (v) dynamic forces, both internally generated as well as externally applied. The three constituents, viz., machine, foundation and soil, contribute to the frequencies of the system. When the system is subjected to dynamic forces (whether internally generated, externally applied, or transmitted through the soil), we get response of the system. If the response is well within the prescribed limits, it is fine; otherwise, it calls for modifications in the system till the response achieved becomes satisfactory. Such a statement is qualitative and its implementation requires complete knowledge of each constituent and experience to precisely identify the modification. At the design stage it is possible to play with the parameters of each constituent to bring down the response under the control limits. However, if such a check/modification is not implemented at the design stage, it may not be that simple to apply desired modifications after the foundation is cast and the machine is placed in position. In either case it may be desirable to know the uncertainties associated with each constituent before one even attempts the design or its modification. An effort is made to broadly identify these uncertainties and address those as given below.

1. Uncertainties Associated with Soil Parameters

There are two distinct types of uncertainties: (i) those associated with the evaluation of dynamic soil parameters; and (ii) those associated with the modeling of soil.

1.1 Dynamic Soil Parameters

It is seen very often that there is a marked variation in the evaluated soil data when evaluation is done by different agencies (Bhatia, 2008). It becomes extremely difficult to precisely choose design dynamic

soil properties from the so-called soil evaluation reports. Such a scenario is practically true for every project site. Level of uncertainty becomes even higher when selecting the dynamic stiffness properties of a group of piles, for application to a machine-foundation system, from the single-pile test. This aspect of soil is also not quantifiable from the point of view of the machine-foundation design. For the design purposes, the author therefore recommends that higher frequency margins of the foundation be kept vis-à-vis the machine operating speed.

1.2 Soil Mass Participation

It is a reality that part of the soil mass vibrates along with the foundation (Barkan, 1962; Bhatia, 2006, 2008; Bhatia and Sinha, 1977; Prakash and Puri, 1988). Some of the issues that need to be addressed are as follows:

- What is the extent of the soil that vibrates with the foundation?
- Does the vibrating soil mass depend upon the mode of vibration?
- Does it have any influence on the soil stiffness and damping?
- Can these aspects be quantified?

There are various opinions expressed by different authors regarding the soil mass participation. According to some, the mass of the soil moving with the foundation varies with the dead load, exciting force, base contact area, mode of vibration, and the type of soil. According to other authors, the size of the participating mass of soil is related to a bulb-shaped stress distribution curve under the effect of uniformly distributed load. Till date no concrete formulation is available giving quantification of the soil mass participation for different types of soils, and what is lacking is perhaps the validation of the results. It is generally the view that soil mass participation will increase the overall effective mass of the machine-foundation system and will thereby tend to reduce the natural frequency. Here again, this aspect of soil is not quantifiable from the point of view of machine-foundation design. For the design purposes, the author therefore recommends (Bhatia, 2008):

- a) for under-tuned foundations, soil mass participation to be ignored; and
- b) for over-tuned foundations, frequency margin to be increased by additional 5%, i.e., natural frequencies to be kept away from the operating speed by 25% instead of the normal 20%.

1.3 Effect of Embedment

All machine foundations are invariably embedded partly into the ground. Many authors have studied this effect and have made varying observations (Barkan, 1962; Bhatia, 2008; Prakash, 1981; Richart et al., 1970; Srinivasulu and Vaidyanathan, 1980; Swami, 1999). Some have reported that embedment causes an increase in the natural frequency, and some have reported that it causes a reduction in amplitudes. By and large, it has been generally agreed that embedment tends to reduce the dynamic amplitudes. The reduction in the amplitudes could be on account of change in stiffness, change in damping, change in soil mass participation, or their combinations. Here again, this aspect of soil is not quantifiable from the point of view of machine-foundation design for all types of soils. For design purposes, the author recommends that it will be on the safe side to ignore the embedment effect while computing the dynamic response.

1.4 Soil Damping

Damping is an inherent property of soil and its influence on forced vibration response is significant during the resonance or near-resonance conditions (Barkan, 1962; Bhatia, 2008; Richart et al., 1970). Different soils exhibit different damping properties, depending upon their soil composition and other characteristic parameters. In the case of embedded foundations, the depth of embedment also influences the damping properties. Soil damping comprises (a) geometrical damping, and (b) material damping. While geometrical damping represents the energy radiated away from the foundation, material damping represents the energy lost within the soil due to the hysteretic effects.

In the context of machine-foundation design, the contribution of geometrical damping to rocking modes of vibration has been reported to be of low order compared to the translational and torsional modes of vibration. Damping in the soil has been observed to be both strain- and frequency-dependent. Same soil exhibits different damping characteristics at different strain levels and similar is the variation with the frequency of excitation. In other words, soil damping not only depends upon the stress, strain, or contact pressure distribution but also on the frequency of vibration. Representation of frequency-dependent soil damping has not found appropriate place in the design industry for real-life design problems (Bhatia,

2008). On the other hand, representation in the form of equivalent viscous damping has found larger acceptability.

It has to be remembered that damping plays a role only during resonance. If one is able to avoid the resonance of foundation with the machine excitation frequencies at the design stage itself, the significance of damping could be felt only during the transient resonance. In the author's opinion, considering strain- and frequency-dependent geometrical or radiation damping in design office practices is not only difficult but inconvenient too. The commonly available mathematical tools with the industry, in general, are not geared to accommodate this type of damping. Further, the use of high-end analytical tools is not recommended for design purposes in view of tight project schedules. In the absence of any specified data for the damping value of a site, the damping coefficient equal to 8% to 10%, i.e., $\zeta = 0.08$ to 0.1 could safely be considered for computing the response at resonance.

2. Uncertainties Associated with Foundation Parameters

Elastic Modulus: The basic question is whether to use the static elastic modulus or dynamic elastic modulus of concrete for design. Some authors and codes of practices recommend the use of dynamic elastic modulus, whereas some suggest the use of static elastic modulus of concrete. The difference is of the order of about 20%. As the dynamic elastic modulus is strain-dependent, and since stresses developed in the foundation during the normal operating conditions are relatively of lower order of magnitude, the author recommends the use of static elastic modulus for dynamic analysis and design (Bhatia, 2008).

Cold Joints, Cracks at Beam Column Interface and Honeycombs: At times cold joints and honeycombs are encountered in the super-structure of a frame foundation. In addition, cracks have also been witnessed at the beam-column interface. Such cracks have a tendency to result in lower stiffness and thereby lower frequencies. Epoxy or cement grout is used for the repair of such cracks. Loss of stiffness on account of this phenomenon is well known but this still remains unquantifiable. In view of this uncertainty, it is recommended to keep slightly higher margins for the over-tuned foundations.

3. Uncertainties Associated with Machine Parameters

Dynamic forces furnished by machine suppliers, at times, contain a fictitious multiplying factor that results in very large dynamic forces (Barkan, 1962; Bhatia, 2006, 2008). This not only makes the life of designer miserable but also adversely affects the reliability of design. It is, therefore, desirable for the designer to evaluate the dynamic forces in line with the balance quality grade of the rotor and to cross-check the same with the given machine data. In addition, phase angle of the dynamic forces pertaining to different rotors may be 180° degree out of phase as shown in Figure 7.

When the forces are 180° out of phase, i.e., $\phi_1 = \phi$ and $\phi_2 = 180 - \phi$, the total maximum reaction along the Y -axis will be $F_{1y} - F_{2y} = F_1 - F_2$ (for $\sin \phi = 1$), and the total maximum reaction along the X -axis will also be $F_{1x} - F_{2x} = F_1 - F_2$ (for $\cos \phi = 1$). In addition, the unbalance forces will give rise to two couples with reference to the moment at any point, say at Bearing 1 (at the distance a , along the Z -axis, from the center of Rotor 1). The maximum value of this moment about the Y -axis is $M_\psi = F_{2x}(L+a) - F_{1x}a$ and about the X -axis is $M_\theta = F_{2y}(L+a) - F_{1y}a$.

This phenomenon is common to practically most of the machines. Thus, the rotational modes of vibration of the foundation get excited and may significantly contribute to the enhanced response. Thus, it is clear that though the generated unbalance forces have components only in the X - and Y -directions, these will also generate moments about the Y - and X -axes. Hence it becomes obvious that it is not enough to compute amplitudes for the vibration modes in the Y - and X -translations; amplitudes must also be computed for the rocking (about the X -axis) as well as the torsional modes (about the Y -axis) for the moments thus generated.

VIBRATION ISOLATION SYSTEM

In machine-foundation design, the term 'isolation' refers to a reduction in the transmission of vibration from machine to the foundation and vice-versa. In other words, it means control of transmission of dynamic forces from machine to the foundation, and thereby to the adjoining structures and equipment,

or from the adjoining structures and equipment to the machine through its foundation (Bhatia, 2008; Bhatia and Sinha, 1977; Prakash, 1981; Singh and Bhatia, 1989; Srinivasulu and Vaidyanathan, 1980).

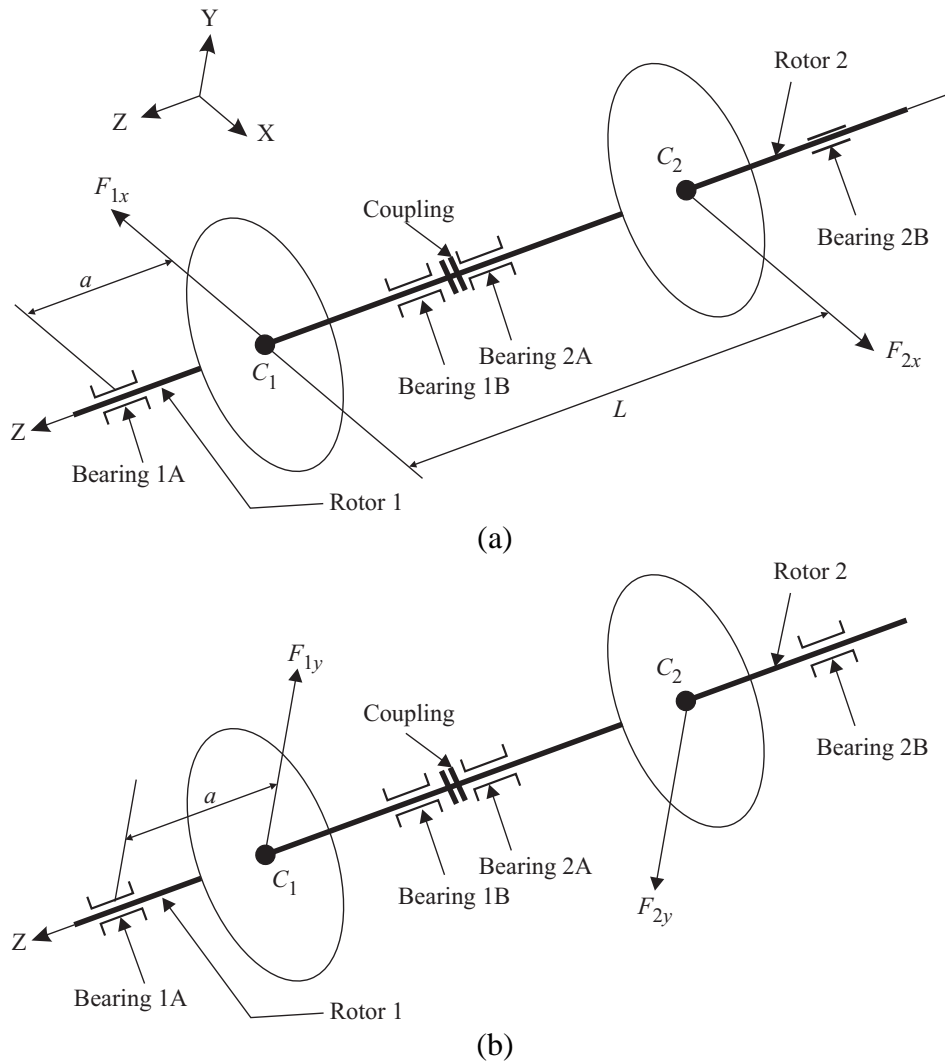


Fig. 7 Machine having two rotors with unbalanced forces out of phase in each rotor: (a) X-component of unbalanced force 180° out of phase; (b) Y-component of unbalanced force 180° out of phase

Principle of Isolation: Whether dynamic excitation is applied at the mass and the force is transmitted at the base of the foundation, or dynamic excitation is applied at the base of the foundation and the force is transmitted at the mass, the transmitted force should be the least. The ratio of the transmitted force to the excitation force is termed as transmissibility ratio (TR). A plot of transmissibility ratio versus frequency ratio is shown in Figure 8.

Isolation Efficiency: Isolation efficiency η is given as $\eta = (1-TR)$. It is clear from this equation that lesser the transmissibility ratio, better is the isolation efficiency η . A plot of isolation efficiency versus frequency ratio is shown in Figure 9.

Isolation Requirements: Generally speaking, for machine-foundation applications one would be interested in the isolation above 85%; otherwise the very purpose of isolation gets defeated. In view of this, let us view the isolation plot for $\eta > 80\%$, which obviously means that $\beta > 2$, as shown in Figure 9. It is noticed from the plot that even for zero damping, one requires $\beta = 3$ for $\eta = 88\%$ and $\beta = 5$ for $\eta = 96\%$. This gives an impression that one can achieve as high isolation as desired just by increasing the frequency ratio. In reality, this impression, however, does not hold any ground. It is evident from Figure 9 that there is hardly any appreciable gain in η for $\beta > 6$, which corresponds to $\eta = 97\%$. This implies

that one can, at best, aim for the isolation efficiency of about $\eta = 97\%$, knowing that the presence of damping in isolators, if any, shall reflect in a reduction of η . It is obvious that higher the value of η , higher will be β and lower will be the frequency of isolation system, $f (= \omega/\beta)$. It is also known that lower the value of f , lower will be the stiffness of the isolation system, k , and that this lower stiffness would result in higher static deflection δ under the self-weight of the system. A plot of isolator system frequency versus static deflection of isolator is shown in Figure 10.

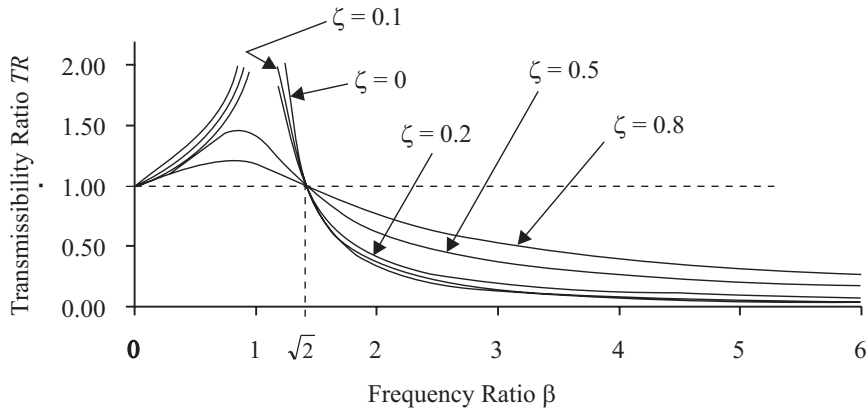


Fig. 8 Transmissibility ratio (TR) versus frequency ratio (β)

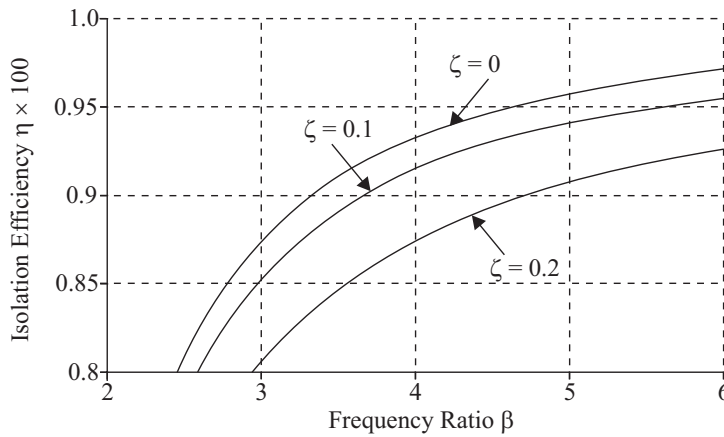


Fig. 9 Isolation efficiency $\eta (> 80\%)$ versus frequency ratio $\beta (> 2)$

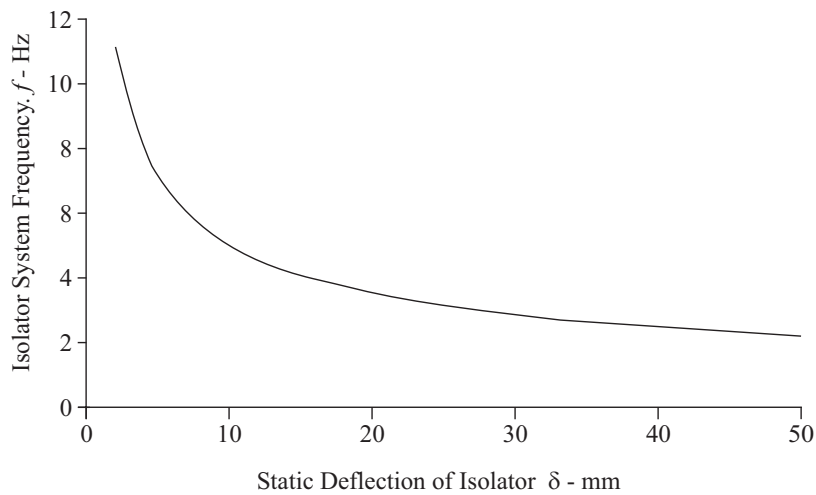


Fig. 10 Isolator system frequency f versus static deflection of isolator unit, δ

Inertia Block: Inertia block, generally made of RCC, is provided to support the machine. It is made heavy enough (with mass two to three times that of the machine) so as to keep the overall centroid in a stable position. It should be rigid enough so as to have its natural frequencies much above the machine speed and its harmonics.

Isolators: These are commercially available devices (as per the required specifications) to be installed between the inertia block and the support system. There are many types of isolators available commercially. We limit our discussions here to only two types: (a) mechanical isolators (spring type with or without damping), and (b) sheet/pad type isolators (cork, rubber sheets, etc).

Selection of Isolator: It is totally dependent on the machine excitation frequency, target isolation efficiency, and the overall mass of machine plus the mass of inertia block. There are many ways one can arrive at the specification for the required isolators. A typical machine system supported on isolators is shown in Figure 11.

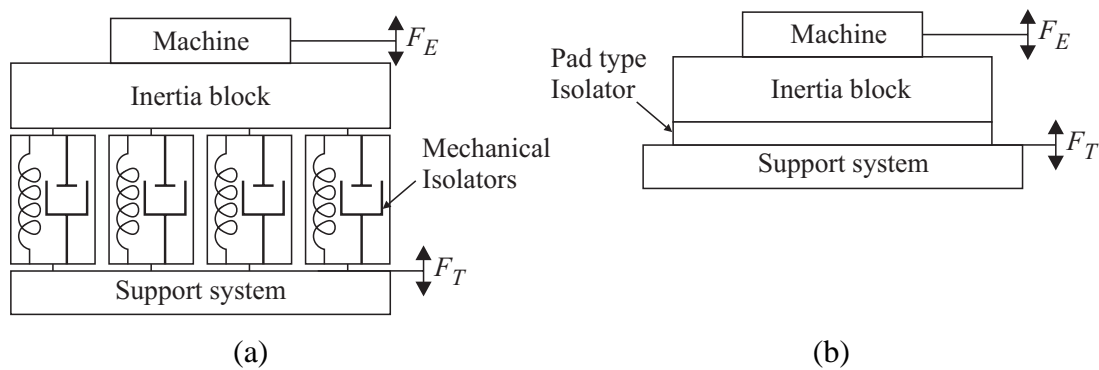


Fig. 11 Machine foundation isolation system: (a) mechanical isolators; (b) sheet/pad type isolators

EARTHQUAKE EFFECTS

Significant damage to machinery has been reported for many earthquake occurrences the world over. Majority of this damage, however, pertains to static electrical/mechanical equipments, and only in rare cases damage is reported for rotating electrical/mechanical equipments. In the context of machine-foundation systems, earthquakes not only influence the foundation but also the machine. Earthquake forces get transmitted from ground to the machines through their foundations.

In the absence of any specific code for earthquake-resistant design of machine-foundation systems, it is recommended to use the provisions of IS 1893 (Part 4) (BIS, 2005). The horizontal seismic coefficient A_h should be computed as per Clause 8.3 of these provisions. Unlike other structures, the author recommends that the vertical seismic coefficient be considered same as the horizontal seismic coefficient in the applications to machine-foundation systems.

Unlike the buildings and structures where ductility plays an important role in bringing down the design seismic coefficient, there is practically no provision for ductility in the design of machine foundation systems. Thus, even controlled damages to the foundations are not permitted. Hence, the seismic coefficient for a machine-foundation system should be computed using the reduction factor $R = 3$, as applicable to the ordinary moment resisting frames (refer Table 3 of IS 1893 (Part 4) (BIS, 2005)). Since the importance factor assigned to a machine varies with the machine functionality or use in the plant cycle, it is recommended to use the same value as that assigned to the industrial structures but not less than 1.5 (refer Table 2 of IS 1893 (Part 4) (BIS, 2005)).

Dynamic interaction between the machines, their foundations, and the soil during the earthquakes is of prime importance. It must be borne in mind that there are no codal provisions to avoid failures of machine-foundation systems during earthquakes. Air gap (or clearance) between the rotor and stator could be as low as 1 to 2 mm and could also be as high as tens of millimeters. The basic objective is that there should not be any rubbing of rotor with the stator. This makes the seismic qualification of machine-foundation systems a shade different from that of the other structural systems. It is recommended to use

the same mathematical model (i.e., the same FE model) as that used for the dynamic analysis of the machine-foundation system under consideration. As mentioned earlier, it must be ensured that the machine is modeled along with the foundation and that its masses are lumped at appropriate centroid locations. It is not only desirable but essential to model the rotor and stator separately. This helps in ensuring the safety against rotor-stator rubbing.

In the event of foundation design requiring structural changes on account of seismic safety, the entire dynamic computations need to be redone. This includes free-vibration analysis, and the analyses for forced-vibration response and transient response, in addition to the analysis for seismic safety.

CONCLUDING REMARKS

This paper is based on the long experience (of about 3 decades) of the author on design, testing and troubleshooting of machine-foundation systems. Salient observations may be made as given below:

1. Generally speaking, machine-foundation design has been associated with the civil engineering discipline. Whether it is a soil specialist or structure specialist, depending upon his/her specialization, the designer studies and analyses all the data connected to his/her specialization and takes the rest of the data as a black box. This is neither desirable nor adequate. This paper recommends a higher level of interaction amongst all the concerned disciplines, which should result in an improved machine performance.
2. The paper highlights various issues related to the mathematical modeling of machine, foundation and soil. The gray areas have been specifically highlighted. The influence of various assumptions and simplifications on the response has also been discussed.
3. From the point of view of dynamic response, limitations of the manual methods of computation have been discussed. It is observed that not only the dynamic behaviour of foundation as a whole but also its elements, viz., beams, columns, pedestals, etc., show strong influence on the machine response.
4. Necessary design aids/methodologies for the modeling and analysis of machine foundations, including various issues related to the mathematical modeling, are provided. Basics of the vibration isolation system for heavy-duty machines are also described.
5. The paper also touches upon the effects of earthquakes on machines as well as on their foundations in view of the reported damages for many industrial systems. Use of commercially available finite element packages, for the analysis and design of foundations, is strongly recommended, but with some caution.

ACKNOWLEDGEMENTS

The author is grateful to two organizations of excellence for work experience, viz., M/s Engineers India Limited (EIL), New Delhi, India and M/s Bharat Heavy Electricals Limited (BHEL), New Delhi, India, for providing him the environment to carry out extensive design-oriented research work including testing and trouble shooting. The author is especially thankful to Mr. R. Venkatesh of EIL, New Delhi, for inducting him into the field of machine foundation as early as in 1971, and to Dr. A.K. Singh of BHEL who had been all along with him in most of the programmes related to machine foundation.

REFERENCES

1. Barkan, D.D. (1962). "Dynamics of Bases and Foundations", McGraw-Hill Book Company, New York, U.S.A.
2. Bhatia, K.G. (1981). "Soil Structure Interaction Effects on the Response of 210 MW TG Frame Foundation", Proceedings of the International Conference on Recent Advances in Geotechnical Earthquake Engineering and Soil Dynamics, St. Louis, U.S.A., Vol. 1, pp. 319–322.
3. Bhatia, K.G. (1984). "Machine Foundation in Power Plant and Other Industries—Case Studies", Proceedings of the International Conference on Case Histories in Geotechnical Engineering, St. Louis, U.S.A., Vol. 2, pp. 775–779.
4. Bhatia, K.G. (2006). "Machine Foundation Design—A State of the Art", Journal of Structural Engineering, SERC, Vol. 33, No. 1, pp. 69–80.

5. Bhatia, K.G. (2008). "Foundations for Industrial Machines—A Handbook for Practising Engineers", D-CAD Publishers, New Delhi.
6. Bhatia, K.G. and Sinha, K.N. (1977). "Effect of Soil-Structure Interaction on the Behaviour of Machine Foundations", Proceedings of the International Symposium on Soil-Structure Interaction, Roorkee, pp. 399–404.
7. BIS (1979). "IS: 2974 (Part IV)-1979—Indian Standard Code of Practice for Design and Construction of Machine Foundations, Part IV: Foundations for Rotary Type Machines of Low Frequency (First Revision)", Bureau of Indian Standards, New Delhi.
8. BIS (1980). "IS: 2974 (Part II)-1980—Indian Standard Code of Practice for Design and Construction of Machine Foundations, Part II: Foundations for Impact Type Machines (Hammer Foundations) (First Revision)", Bureau of Indian Standards, New Delhi.
9. BIS (1982). "IS: 2974 (Part I)-1982—Indian Standard Code of Practice for Design and Construction of Machine Foundations, Part I: Foundation for Reciprocating Type Machines (Second Revision)", Bureau of Indian Standards, New Delhi.
10. BIS (1987). "IS: 2974 (Part 5)-1987—Indian Standard Code of Practice for Design and Construction of Machine Foundations, Part 5: Foundations for Impact Machines other than Hammer (Forging and Stamping Press, Pig Breaker, Drop Crusher and Jolter) (First Revision)", Bureau of Indian Standards, New Delhi.
11. BIS (1992). "IS 2974 (Part 3): 1992—Indian Standard Design and Construction of Machine Foundations—Code of Practice, Part 3: Foundations for Rotary Type Machines (Medium and High Frequency) (Second Revision)", Bureau of Indian Standards, New Delhi.
12. BIS (2005). "IS 1893 (Part 4): 2005—Indian Standard Criteria for Earthquake Resistant Design of Structures, Part 4: Industrial Structures Including Stack-like Structures", Bureau of Indian Standards, New Delhi.
13. Major, A. (1980). "Dynamics in Civil Engineering—Analysis and Design, Vols. I–IV", Akadémiai Kiadó, Budapest, Hungary.
14. Prakash, S. (1981). "Soil Dynamics", McGraw-Hill Book Company, New York, U.S.A.
15. Prakash, S. and Puri, V.K. (1988). "Foundations for Machines: Analysis and Design", John Wiley & Sons, New York, U.S.A.
16. Ramdasa, K., Singh, A.K. and Bhatia, K.G. (1982). "Dynamic Analysis of Frame Foundation Using FEM", Proceedings of the 7th Symposium on Earthquake Engineering, Roorkee, Vol. 1, pp. 411–416.
17. Richart Jr., F.E., Hall Jr., J.R. and Woods, R.D. (1970). "Vibrations of Soils and Foundations", Prentice-Hall, Englewood Cliffs, U.S.A.
18. Singh, A.K. and Bhatia, K.G. (1989). "Base Isolation of Equipment and System", Bulletin of Indian Society of Earthquake Technology, Vol. 26, No. 4, pp. 39–48.
19. Srinivasulu, P. and Vaidyanathan, V. (1980). "Handbook of Machine Foundations", Tata McGraw-Hill Publishing Company, New Delhi.
20. Swami, S. (1999). "Soil Dynamics and Machine Foundation", Galgotia Publications Private Limited, New Delhi.

NUMERICAL ANALYSIS OF PERFORMANCE OF SOIL NAIL WALLS IN SEISMIC CONDITIONS

G.L. Sivakumar Babu and Vikas Pratap Singh

Department of Civil Engineering
Indian Institute of Science
Bangalore-560012

ABSTRACT

Evidences from the field and full-scale laboratory tests suggest that soil nail walls perform remarkably well under seismic conditions. In this study an attempt has been made to study the performance of a soil nail wall supporting a vertical cut of 8 m height under seismic conditions. The wall is designed in conventional manner by using the allowable stress design procedure. The response of the wall is then simulated numerically by using a finite element analysis. Seismic data from Bhuj and Uttarkashi earthquakes is used for the pseudo-static and dynamic analyses. To assess the performance of the soil nail wall, parameters such as maximum lateral displacements, development of nail forces, important failure modes of soil nail walls, have been studied under both static and seismic conditions. Results of the numerical analyses indicate that the use of soil nail walls is desirable to impart stability to the retaining systems under seismic conditions.

KEYWORDS: Soil Nailing, Conventional Design, Seismic Performance, Numerical Analysis

INTRODUCTION

In areas of high seismic activity, earthquake effects on the stability of retaining walls assume considerable importance, and soil nail walls are considered as useful options in this context. A review of literature shows that soil nail walls have performed well during strong ground motions in contrast with the generally poor performance of gravity retaining structures. After the 1989 Loma Prieta, 1995 Kobe, and 2001 Nisqually earthquakes, it was reported that soil nail walls showed no sign of distress or significant permanent deflection, despite having experienced, in some cases, ground accelerations as high as 0.7g (Felio et al., 1990; Tatsuoka et al., 1996). These observations indicate that soil nail walls appear to have an inherent satisfactory seismic response. This has been attributed to the intrinsic flexibility of soil-nailed systems (which is comparable to that of other flexible retaining systems, such as MSE walls) and possibly to some levels of conservatism in the existing design procedures. Similar trends have been obtained from centrifuge tests performed on reduced-scale models of soil nail walls (e.g., Vucetic et al., 1993; Tufenkian and Vucetic, 2000). However, any detailed analysis on the performance of soil nail walls is not brought out in the above studies. It is also desirable that a detailed numerical analysis is conducted with regard to the application of the technique in Indian context using appropriate earthquake data. The results presented in this paper fulfill this requirement.

In this study, a typical soil nail wall of 8 m height, that is representative of typical heights of retaining walls, is designed in conventional manner by using the allowable stress design approach presented in the Federal Highway Administration report for analyses, design and construction of soil nail walls (Lazarte et al., 2003). The external failure modes of soil nail walls namely, global stability and sliding stability, are studied under static, pseudo-static, and dynamic conditions. Plaxis (2002), a two-dimensional finite element based computational tool, is used for numerical simulation of the (conventionally designed) soil nail wall and for studying its stability under static and seismic conditions. Additionally, influence of seismicity on nail forces, maximum horizontal displacements, and important internal failure modes such as nail pullout failure and nail tensile strength failure, is also studied and compared under static and seismic conditions. Table 1 shows the recommended minimum factors of safety, modified after Byrne et al. (1998), for design of permanent soil nail walls based on the allowable stress design (ASD) method, where loads are unfactored.

Table 1: Minimum Recommended Factors of Safety for Permanent Soil Nail Walls

Failure Mode	Resisting Component	Symbol	Minimum Recommended Factors of Safety	
			Seismic	Static
External stability	Global stability	FS_G	1.10	1.5
	Sliding	FS_{SL}	1.10	1.5
Internal stability	Pull-out resistance	FS_P	1.50	2.0
	Nail bar tensile strength	FS_T	1.35	1.8
Facing failure	Facing flexure	FS_{FF}	1.10	1.5
	Facing punching failure	FS_{FP}	1.10	1.5

MATERIAL PROPERTIES AND DESIGN PARAMETERS

It is assumed that the in-situ ground constitutes a deposit of sandy soil. Terrain is considered to be generally flat and the elevation of ground water table is significantly below the bottom of the soil nail wall. Table 2 shows the material properties and other design parameters adopted for the study. For dynamic simulations, the January 26, 2001 Bhuj earthquake record at Ahmedabad and October 20, 1991 Uttarkashi earthquake record at Uttarkashi (Shrikhande, 2001) are used.

Table 2: Material Properties and Other Parameters Adopted for the Conventional Design

Parameter	Value
Vertical height of wall, H (m)	8.0
Face batter, α' (degree)	0.0
Slope of backfill, β (degree)	0.0
Wall-soil interface friction angle, δ (degree)	15.0
Cohesion, c (kPa)	1.0
Friction angle, $\phi (= \phi')$ (degree)	30.0
Unit weight, γ (kN/m ³)	16.0
Modulus of elasticity of soil, E_s (MPa)	20.0
Yield strength of nail, f_y (MPa)	415
Modulus of elasticity of nail, E_n (GPa)	200.0
Nail spacing, $S_v \times S_H$ (m×m)	1.0×1.0
Nail inclination (with horizontal), i (degree)	15.0
Drill hole diameter, D_{DH} (mm)	100.0
Compressive strength of grout, f_{ck} (MPa)	20.0
Ultimate bond strength, q_u (kPa)	100.0
Modulus of elasticity of grout, E_g (GPa)	22.0
Horizontal seismic coefficient, k_h	0.106
Vertical seismic coefficient, k_v	0.0

CONVENTIONAL DESIGN

The conventional design of the soil nail wall is carried with reference to the allowable stress design procedure stated in the report of Federal Highway Administration for analyses, design and construction of soil nail walls (Lazarte et al., 2003). The design is carried out in two stages: (i) preliminary design, and (ii) final design.

1. Preliminary Design

The preliminary design involves use of simplified design charts and tables to arrive at the design nail length and diameter. Following are the general steps in the preliminary design:

- a) For the specific project application, obtain general parameters such as face batter α , back slope β , effective friction angle ϕ' , and ultimate bond strength q_u , and calculate the normalized allowable pullout resistance μ using Equation (1):

$$\mu = \frac{q_u D_{DH}}{FS_p \gamma S_H S_V} \quad (1)$$

- b) From the relevant design chart, obtain the normalized length L/H and normalized force $t_{\max-s}$.
- c) Evaluate and apply suitable correction factors to the L/H ratio and $t_{\max-s}$ values obtained in the previous step for the drill hole diameter other than 100 mm, normalized cohesion value c^* other than 0.02, and global factor of safety other than 1.35.
- d) Determine the maximum design load in the nail, $t_{\max-s}$, (in kN) using the value of corrected $t_{\max-s}$ as in Equation (2), and calculate the required cross-sectional area of the nail bar, A_t , from Equation (3):

$$T_{\max-s} = t_{\max-s} \gamma H S_H S_V \quad (2)$$

$$A_t = \frac{T_{\max-s} FS_T}{f_y} \quad (3)$$

- e) Finally select the closest commercially available bar size that has a cross-sectional area at least equal to A_t , as evaluated in the previous step.

2. Final Design

The final design includes analysis of external failure modes (such as global stability and sliding stability), analysis of internal failure modes (such as nail pullout failure and nail tensile strength failure), design of permanent facing and verification of important facing failure modes (such as facing flexure failure and facing punching shear failure), and influence of other site-specific considerations, such as seismic loading, on global and sliding stability. In the present study only the important external and internal failure modes are considered to assess and compare the performance of the (conventionally designed) soil nail wall under static and seismic conditions.

According to the conventional design procedure used in this study, whenever seismic considerations are involved, a pseudo-static approach is adopted for determining the factor of safety for global stability, FS_G , and factor of safety for sliding stability, FS_{SL} . However, the global stability analysis (for FS_G) is generally carried out by using a computational tool for slope stability, and major emphasis is laid on the selection of suitable seismic acceleration coefficients (k_h and k_v). While analyzing the sliding stability (for FS_{SL}) of a soil nail wall under seismic loads, the total active thrust P_{AE} during an earthquake due to the earth pressures behind the soil block must be considered. This force is a combination of the static and dynamic active lateral earth pressures that are induced by the inertial forces. The lateral earth force, including the seismic effects, is evaluated using the Mononobe-Okabe (M-O) method, which is an extension of the Coulomb theory (Kramer, 2005). Table 3 presents a summary of important design variables determined for the soil nail wall based on the conventional design procedure.

Table 3: Summary of Conventional Design Results

Design Variable	Value
Nail length, L_N (m)	4.70
Nail diameter, d (m)	16.0
Maximum axial force in nail, $T_{\max-s}$ (kN)	32.56
Axial force at nail head, T_o (kN)	19.53
Pullout capacity of nail per unit length, Q_u (kN/m)	31.41
Maximum axial tensile load capacity of nail, R_T (kN)	83.44
Factor of safety against pullout (on ultimate bond strength), FS_p	2.00
Factor of safety against nail tensile strength, FS_T	2.56
Factor of safety against global stability, FS_G	1.56 (1.11)
Factor of safety against sliding stability, FS_{SL}	2.21 (1.74)
Facing	Permanent cast in-place R.C.C. facing 200 mm thick
Note: Figures in bracket indicate the corresponding values from seismic considerations (with k_h and k_v taken as 0.106 and 0.0, respectively)	

In Table 3, the maximum axial force $T_{\max-s}$ is calculated from Equation (2), whereas the axial force at the nail head, T_o , is given by Equation (4). Based on the measurements of forces in nails at the head, the nail head force, T_o , is expressed as

$$T_o = T_{\max-s} \left[0.6 + 0.2(S_v [m]) - 1 \right] \quad (4)$$

The pullout capacity per unit length, Q_u (also referred to as the load transfer rate capacity), is given by Equation (5):

$$Q_u = \pi q_u D_{DH} \quad (5)$$

The maximum axial tensile load capacity of a nail, R_T , is given by Equation (6):

$$R_T = A_t f_y \quad (6)$$

The factor of safety against the nail pullout failure, FS_p , is calculated as the ratio of pullout capacity R_p of the nail to the maximum axial force developed in the nail, i.e.,

$$FS_p = \frac{R_p}{T_{\max-s}} = \frac{Q_u L_p}{T_{\max-s}} \quad (7)$$

where, L_p is the pullout length of the nail. The factor of safety against the nail tensile strength failure, FS_T , is calculated as the ratio of maximum axial tensile load capacity of the nail to the maximum axial force developed in the nail, i.e.,

$$FS_T = \frac{R_T}{T_{\max-s}} \quad (8)$$

The factor of safety against the global failure, FS_G , is expressed as the ratio of the sum of resisting forces, ΣR , and the sum of driving forces, ΣD , which act tangent to the potential failure plane:

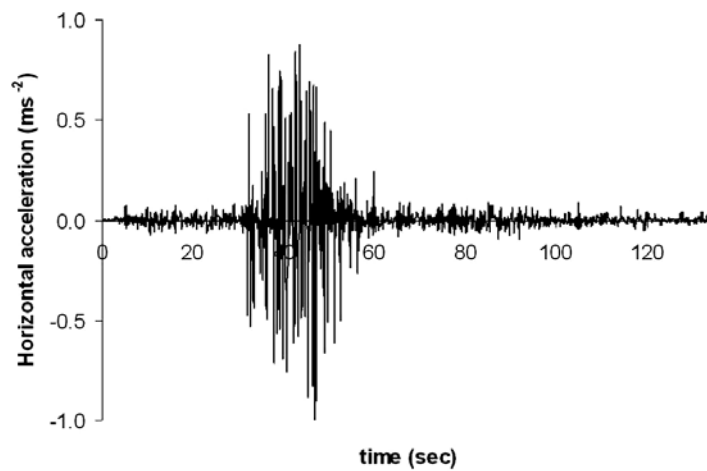
$$FS_G = \frac{\Sigma R}{\Sigma D} \quad (9)$$

Similarly, the factor of safety against the sliding failure, FS_{SL} , is expressed as the ratio of the sum of the resisting forces, ΣR , and the sum of the driving forces, ΣD , which act along the potential horizontal sliding failure plane at the base of the soil nail wall:

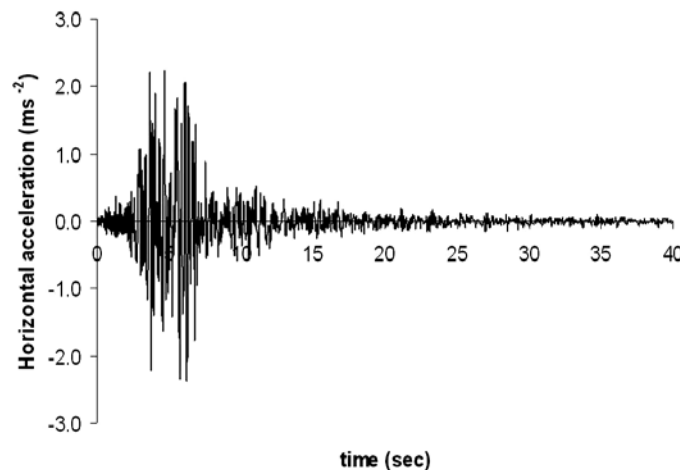
$$FS_{SL} = \frac{\Sigma R}{\Sigma D} \tag{10}$$

NUMERICAL SIMULATION

As stated earlier, Plaxis (2002) is used for simulating and analyzing the response of soil nail wall under static and seismic conditions. Numerical modelling is carried out assuming the plane strain state of stresses. The 15-node triangular elements with medium mesh density are used for the finite element discretization. The in-situ soil is simulated as Mohr-Coulomb (MC) material for the static and pseudo-static analyses and as hardening soil with small-strain stiffness (HSS) for the dynamic analyses. Various inputs parameters for the HSS model are judiciously adopted from the manual of Plaxis (2002) after calibration for the Houston sand. The advantage of using HSS model is that it accounts for the increased stiffness of soils at small strains (Benz, 2007). For the dynamic analyses, strong motion records, as shown in Figures 1(a) and 1(b) for the 2001 Bhuj and 1991 Uttarkashi earthquakes respectively, are used. Soil nails and wall facing are simulated as the linear elastic materials. Plate elements are used to model the nails and facing. Figures 2(a) and 2(b) show the outline and finite element model of the 8-m high vertical soil nail wall. Construction sequences are simulated as the staged construction with 2-m excavation lift in each stage.

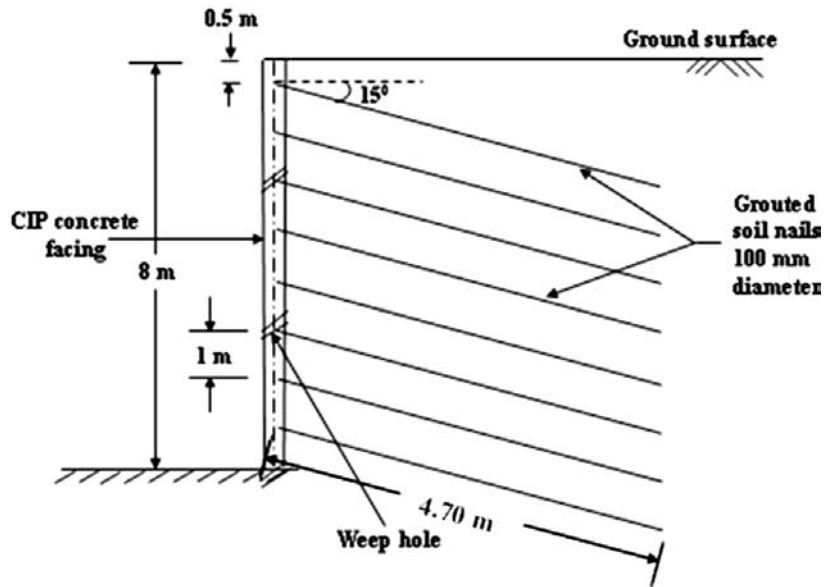


(a)

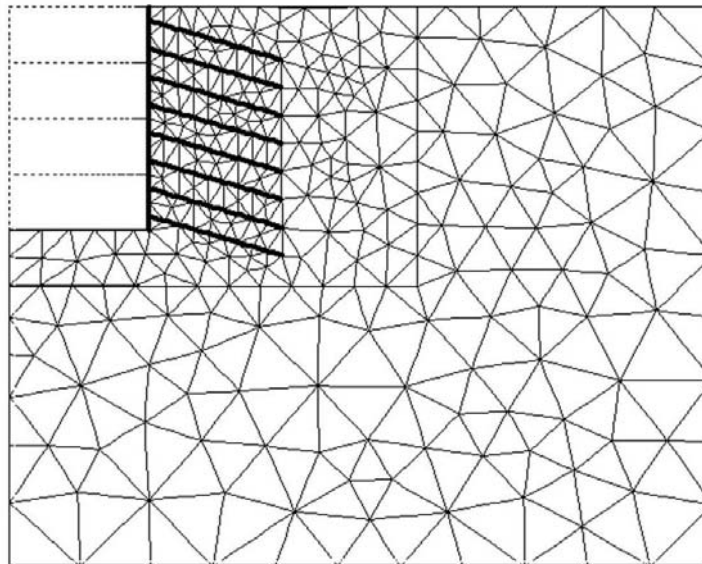


(b)

Fig. 1 Strong motion records for the Bhuj and Uttarkashi earthquakes: (a) Bhuj earthquake record at Ahmedabad; (b) Uttarkashi earthquake record at Uttarkashi



(a)



(b)

Fig. 2 Soil nail wall supporting the 8-m high vertical cut: (a) outline of the designed soil nail wall; (b) the numerically modelled state

Numerical simulations are conducted for various parameters to assess the performance of soil nail wall system under static, pseudo-static, and dynamic conditions. Table 4 presents a summary of some of the important results obtained. For determination of factors of safety against the internal failure modes (i.e., the nail pullout failure and the nail tensile strength failure), the corresponding values of $T_{\max-s}$ obtained from the numerical simulations are used in Equations (7) and (8).

The strength reduction technique (also known as the phi-c reduction technique (Matsui and San, 1992)) is typically used for the determination of factor of safety in numerical analysis in geotechnical engineering. In this technique, the strength parameters “ $\tan \phi$ ” and “cohesion c ” of the soil are successively and simultaneously reduced until failure of the structure occurs. Though this method is advantageous (Dawson et al., 1999) as it identifies the critical failure mechanism automatically, which is generally assumed in the conventional analysis, it excludes the stress-dependent stiffness behavior and hardening effects of the soil. To circumvent the above difficulty and to obtain the factors of safety corresponding to the results of dynamic analyses, a regression analysis procedure is used. To obtain the relationship between the global factor of safety and the maximum displacement (for the determination of global factor of safety), several numerical simulations of the soil nail wall are carried out for the static

case by varying the values of cohesion c and friction angle ϕ . The results are presented and discussed in the following sections.

Table 4: Summary of the Results of Numerical Simulations

Analysis Parameter	Analysis				
	Static	Pseudo-Static		Dynamic	
		Bhuj	Uttarkashi	Bhuj	Uttarkashi
Horizontal seismic coefficient, k_h	--	0.106	0.241	--	--
Vertical seismic coefficient, k_v	--	0.00	0.00	--	--
Maximum axial force in nail, $T_{\max-s}$ (kN)	22.34	34.50	40.73	34.98	33.06
Maximum axial force at nail head, T_o (kN)	19.96	27.80	32.46	29.17	28.86
Maximum horizontal displacement of soil nail wall (%)	0.61	3.29	5.24	1.13	0.82
Factor of safety against global stability, FS_G	1.23	0.95	0.81	1.10	1.17
Factor of safety against nail pullout failure, FS_p	1.78	1.15	0.98	1.14	1.21
Factor of safety against nail tensile strength failure, FS_T	3.73	2.42	2.05	2.38	2.52

RESULTS AND DISCUSSION

Important results of the conventional design and the numerical simulations (for the static and seismic conditions) of the soil nail wall are summarized in Tables 3 and 4, respectively. It is evident from the factor of safety values for the important failure modes considered in the present study that the soil nail wall is stable under the static as well as seismic conditions used for the analyses.

To study the response of dams under dynamic conditions, Sivakumar Babu and Rao (2005) obtained a regression relationship between the global factor of safety and the maximum displacement obtained from the dynamic analyses. To obtain this relationship, the use of phi-c reduction technique was made. A similar procedure is adopted in this paper. For the static case with actual soil strength parameters (i.e., cohesion $c = 1$ kPa, friction angle $\phi = 30^\circ$) a factor of safety value of 1.23 is obtained. This value according to the phi-c reduction technique corresponds to reduced values of strength parameters (i.e., cohesion $c = 0.83$ kPa, friction angle $\phi = 25.51^\circ$), resulting in a factor of safety value equal to unity. Hence, by varying the soil strength parameters between the actual and reduced values, factor of safety values and the corresponding horizontal displacements are obtained. Finally, a power law is fitted, as shown in Figure 3, between the factor of safety and the maximum horizontal displacement, with an r -square value of 0.9714 indicating a good correlation, and is given by Equation (11):

$$FS_G = 2.7346(h_x)^{-0.2013} \tag{11}$$

where, FS_G denotes the global factor of safety and h_x the maximum horizontal displacement (in mm).

It may be noted that the values of global factor of safety FS_G (see Table 4) obtained from the pseudo-static analyses are less in comparison to those obtained from the dynamic analyses using actual time history data for the earthquakes. This is due to the limitation of the pseudo-static approach, which assumes that the earthquake force acts continuously on the wall, whereas time history data of the earthquake shows that the earthquake force acts for a short duration. The duration of strong ground motion can have a strong influence on the damage caused by an earthquake. A motion of short duration may not produce enough load reversals for damaging response to build up in a structure, even if the amplitude of the motion is high. On the other hand, a motion with moderate amplitude but long duration can produce several load reversals to cause substantial damage (Kramer, 2005).

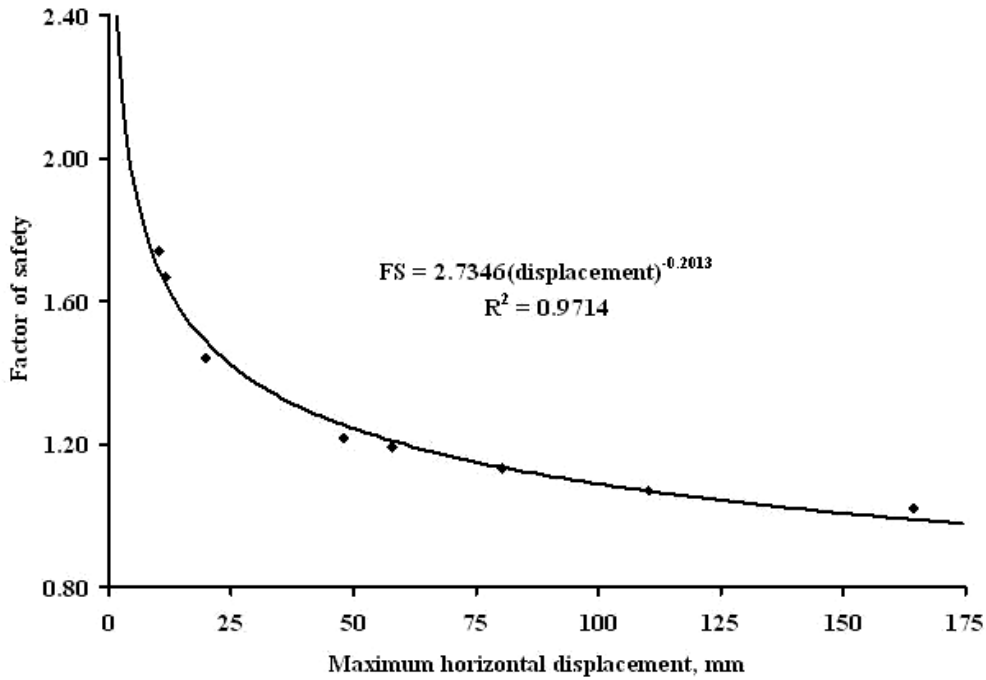


Fig. 3 Relation between the global factor of safety and the displacement of the soil nail wall

The factors of safety values in Table 4 show higher values of factor of safety for the Uttarkashi earthquake motion that has higher ground accelerations and shorter strong motion duration (equal to 8 s) in comparison to the smaller factor of safety values for the Bhuj earthquake motion with lesser amplitudes of ground accelerations and longer strong motion duration (equal to 25 s). This trend in the factor of safety values is in accordance with the above explanation and hence justifies the factor of safety values given in Table 4. Thus, it may be stated that the soil nail wall is stable under static and seismic conditions and fulfills the minimum recommended values (see Table 1), as necessary for the stability of the permanent soil-nailed structures.

Theoretically, the average maximum tensile force in the nails of the wall is calculated as $T_{\max} = K_a \gamma H S_V S_H$. However, the tensile force in the lower portion of the wall decreases considerably to approximately 50 percent of the value in the upper part. Alternatively, Briaud and Lim (1997) suggest that the average maximum in-service tensile force in the top row of the soil nails can be calculated as $T_{\max} = 0.65 K_a \gamma H S_V S_H$. For the subsequent soil nail rows, Briaud and Lim (1997) also suggest that the maximum in-service tensile force is only half of the force in the upper nails. Figures 4(a) and 4(b) show similar trends in the variation of maximum axial force in the nails with the depth of inclusion. Those illustrate that the average in-service nail force is smaller than that calculated by considering the full active earth lateral pressure distribution.

According to Juran (1985), the maximum lateral displacement of the soil nail walls does not generally exceed 0.2% of the vertical height. Additionally, according to the conventional design procedure adopted in present study, for a vertical soil nail wall with sandy soil behind, the maximum horizontal displacements at the top of the wall should not exceed 1/500 of the wall height. From the numerical simulations under the static and seismic conditions, it is observed that the displacement values of soil nail wall do not satisfy the maximum displacement limitations. Figures 5(a) and 5(b) show a comparison of the maximum horizontal displacement of the soil nails with the depth of embedment, as obtained from the static, pseudo-static and dynamic simulations of the soil nail wall. It is evident that the pseudo-static analyses predict very conservative estimates of the displacements.

The trends in the development of bending moments and shear forces in nails obey the established research findings. Compared to the axial forces, development of the bending moments and shear forces in nails is not significant. Elias and Juran (1991) have found that the shear and bending nail strengths contribute less than 10 percent to the overall stability of the wall. Due to this relatively modest contribution, the shear and bending strengths of the soil nails are conservatively disregarded in the conventional design procedure.

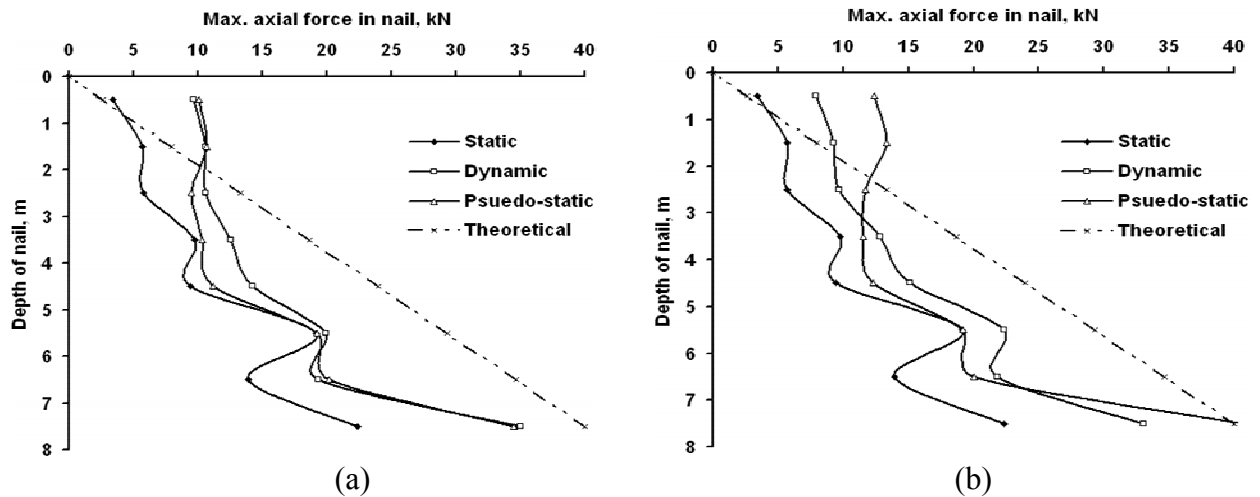


Fig. 4 Development of the maximum (tensile) axial force in nails with the depth of embedment for (a) the Bhuj earthquake record at Ahmedabad, and (b) the Uttarkashi earthquake record at Uttarkashi

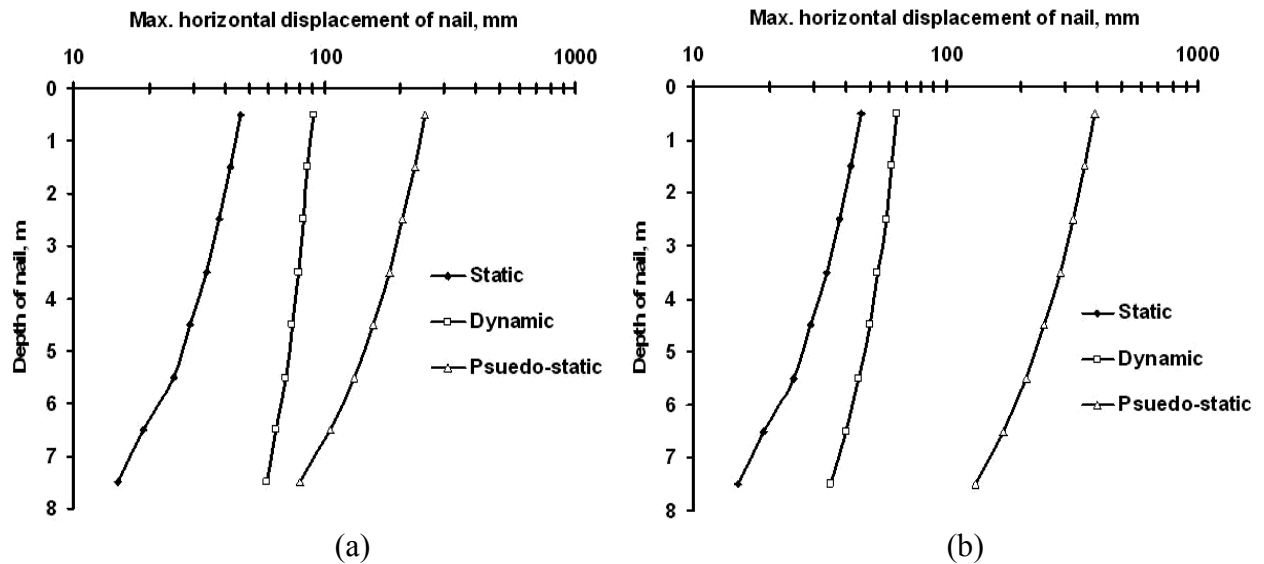


Fig. 5 Variation of the maximum horizontal displacement of nails with the depth of embedment for (a) the Bhuj earthquake record at Ahmedabad, and (b) the Uttarkashi earthquake record at Uttarkashi

CONCLUSIONS

In the present study, the stability of a typical soil nail wall under seismic conditions has been examined using the conventional FHWA procedure and via numerical simulations. An overview of the various important failure modes suggests that the factor of safety values obtained conventionally as well as from the numerical simulations for different cases (i.e., static, pseudo-static and dynamic) satisfy the corresponding minimum recommended values. This implies that the soil nail wall under consideration is stable under the seismic conditions similar to those used in the present study. This is in accordance with the previous research findings about the performance of soil nail walls in seismic conditions. It has been also observed that the pseudo-static analyses result in conservative estimates of displacements and factor of safety values compared to those obtained from the time histories of the considered earthquake motions. The results show that the soil nailing technique provides a feasible, efficient, and economical alternative to the conventional retaining structures under seismic conditions, particularly for supporting vertical or near vertical cuts made in soil for various slope stability applications in geotechnical engineering.

ACKNOWLEDGEMENTS

The authors thank the reviewers for their constructive criticism and useful comments. The work presented in this paper is a part of the research project, “Guidelines for Soil Nailing Technique in Highway Engineering (R-86)” financed by the Ministry of Shipping, Road Transport and Highways, India. The authors express thanks to the Ministry for funding and providing necessary support for the project. The authors also express their thanks to Department of Earthquake Engineering, Indian Institute of Technology Roorkee for providing the strong motion records used in this study.

REFERENCES

1. Benz, T. (2007). “Small-Strain Stiffness of Soils and Its Numerical Consequences”, Ph.D. Thesis, Institut für Geotechnik, Universität Stuttgart, Germany.
2. Briaud, J.L. and Lim, Y. (1997). “Soil-Nailed Wall under Piled Bridge Abutment: Simulation and Guidelines”, *Journal of Geotechnical and Geoenvironmental Engineering*, ASCE, Vol. 123, No. 11, pp. 1043–1050.
3. Byrne, R.J., Cotton, D., Porterfield, J., Wolschlag, C. and Ueblacker, G. (1998). “Manual for Design and Construction Monitoring of Soil Nail Walls”, Report FHWA-SA-96-69R, Federal Highway Administration, U.S. Department of Transportation, Washington, DC, U.S.A.
4. Dawson, E.M., Roth, W.H.A. and Drescher, A. (1999). “Slope Stability Analysis by Strength Reduction”, *Geotechnique*, Vol. 49, No. 6, pp. 835–840.
5. Elias, V. and Juran, I. (1991). “Soil Nailing for Stabilization of Highway Slopes and Excavations”, Report FHWA-RD-89-198, Federal Highway Administration, U.S. Department of Transportation, Washington, DC, U.S.A.
6. Felio, G.Y., Vucetic, M., Hudson, M., Barar, O. and Chapman, R. (1990). “Performance of Soil Nailed Walls during the October 17, 1989 Loma Prieta Earthquake”, *Proceedings of the 43rd Canadian Geotechnical Conference*, Quebec, Canada, Vol. 1, pp. 165–173.
7. Juran, I. (1985). “Reinforced Soil Systems—Application in Retaining Structures”, *Geotechnical Engineering*, Vol. 16, No. 1, pp. 39–81.
8. Kramer, S.L. (2005). “Geotechnical Earthquake Engineering”, Pearson Education, Singapore.
9. Lazarte, C.A., Elias, V., Espinoza, R.D. and Sabatini, P.J. (2003). “Geotechnical Engineering Circular No. 7—Soil Nail Walls”, Report FHWA0-IF-03-017, Federal Highway Administration, U.S. Department of Transportation, Washington, DC, U.S.A.
10. Matsui, T. and San, K.C. (1992). “Finite Element Slope Stability Analysis by Shear Strength Reduction Technique”, *Soils and Foundations*, Vol. 32, No. 1, pp. 59–70.
11. Plaxis (2002). “PLAXIS 2D: Reference Manual, Version 8.0”, Plaxis BV, Delft, The Netherlands.
12. Shrikhande, M. (editor) (2001). “Atlas of Indian Strong Motion Records: CD-ROM”, Department of Earthquake Engineering, Indian Institute of Technology Roorkee, Roorkee.
13. Sivakumar Babu, G.L. and Rao, R.S. (2005). “Analysis of Earthquake Induced Displacements of Embankments”, *Indian Geotechnical Journal*, Vol. 35, No. 4, pp. 349–364.
14. Tatsuoka, F., Koseki, J. and Tateyama, M. (1996). “Performance of Reinforced Soil Structures during the 1995 Hyogo-ken Nanbu Earthquake”, *Proceedings of the International Symposium on Earth Reinforcement*, Fukuoka/Kyushu, Japan, Vol. 2, pp. 973–1008.
15. Tufenkjian, M.R. and Vucetic, M. (2000). “Dynamic Failure Mechanism of Soil-Nailed Excavation Models in Centrifuge”, *Journal of Geotechnical and Geoenvironmental Engineering*, ASCE, Vol. 126, No. 3, pp. 227–235.
16. Vucetic, M., Tufenkjian, M. and Doroudian, M. (1993). “Dynamic Centrifuge Testing of Soil-Nailed Excavations”, *Geotechnical Testing Journal*, Vol. 16, No. 2, pp. 172–187.